A LOOK INTO THE DEVELOPMENT OF REAL-TIME SHAPE-CHANGING DNA ORIGAMI

by

Sally Farag
A Thesis
Submitted to the
Graduate Faculty
of
George Mason University
in Partial Fulfillment of
The Requirements for the Degree
of
Master of Science
Bioengineering

Committee:

_____ Dr. Rémi Veneziano, Thesis Director

_____ Dr. Eugene Kim, Committee Member

_____ Dr. Barney Bishop, Committee Member

_____ Dr. Kim Blackwell, Department Chair

Date: _____7/28/2023_____ Summer Semester 2023
George Mason University
Fairfax, VA

A Look into the Development of Real-Time Shape-Changing DNA Origami

A Thesis submitted in partial fulfillment of the requirements for the degree of Master of Science at George Mason University

by

Sally Farag
Bachelor of Science
George Mason University, 2023

Director: Rémi Veneziano, Assistant Professor
Department of Bioengineering

Summer Semester 2023
George Mason University
Fairfax, VA

DEDICATION

After Al-‘Aleem, I dedicate this work to my grandparents, mother, and siblings. They have always supported me and been by my side. Peace and blessings be upon you all.

ACKNOWLEDGEMENTS

The first thanks, praises, and appreciations are in the name of the Entirely Merciful, the Especially Merciful.

I would like to thank Dr. Rémi Veneziano for all the guidance and support that he provided throughout the past few years and throughout the development and research of this work. I am very grateful to have had him as a professor and advisor. I also give much of my deep thanks and appreciation to Dr. Shrishti Singh and Dr. Esra Oktay for mentoring me in the lab and teaching me how to conduct several experiments and use many different machines. I would also like to thank Carolina Gomes, Dylan Scarton, and Sean Hu for always being there whenever I had questions and engaging in numerous helpful discussions. Additionally, I would like to thank Angelica Galvan and Christopher Green for the AFM images I obtained in this research.

Lastly, I would like to thank my family, friends, and colleagues for all of their encouragement and support. Thank you for being by my side.

TABLE OF CONTENTS

LIST OF TABLES

LIST OF FIGURES

LIST OF EQUATIONS

LIST OF ABBREVIATIONS AND SYMBOLS

Folding Buffer ..... FB
Phosphate Buffered Saline ..... PBS
Triangle ..... Tri
Tetrahedron ..... Tet
Crescent ..... Cres
FRET Efficiency ..... E
Donor Intensity ..... I_D
Donor-Acceptor Intensity ..... I_{DA}
Polymerase Chain Reaction ..... PCR
Asymmetric Polymerase Chain Reaction ..... aPCR
Nanometer ..... nm
Micromolar ..... µM
Nanomolar ..... nM
Tris-acetate Buffer ..... TAE
Atomic Force Microscopy ..... AFM
Dynamic Light Scattering ..... DLS
Base Pair ..... BP

ABSTRACT

A LOOK INTO THE DEVELOPMENT OF REAL-TIME SHAPE-CHANGING DNA ORIGAMI

Sally Farag, M.S.

George Mason University, 2024

Thesis Director: Dr. Rémi Veneziano

DNA origami is the art of folding DNA molecules into prescribed nanostructures that may be used as nanocarriers for various applications such as drug and vaccine delivery. These DNA origami structures are assembled with two different types of DNA strands: one long single-stranded DNA scaffold strand, and several short oligonucleotides, called the staple strands. While there have been many advancements in this field, with notably the synthesis of actuatable nanoparticles, little is known on how to design shape-changing DNA origami. This type of structure could be used to trigger specific biological mechanisms by releasing or presenting biomolecules upon specific stimuli such as pH, biomolecules (e.g., RNA or cytokines), or temperature. This research focuses on applying DNA origami design concepts to construct multiple DNA nanoparticles with the same single-stranded scaffold strand. These nanoparticles would only have a few variations in the staple strands used to allow quick shape-changing by replacing only a few strands.

Complex structures of DNA nanoparticles can be assembled with multiple smaller origami structures that act as building-blocks pieced together and can be reorganized to provide fast shape-changes. As such, before designing the final nanoparticle structures in TIAMAT, a tetrahedron was designed to serve as their building-block, allowing for a more cohesive build and transition between each nanoparticle. Through this method, two different nanoparticle structures were designed, each containing three of the tetrahedrons: a triangular structure and a crescent structure. Both were made using the same 1,632 nucleotides scaffold strand, demonstrating that designing multiple structures from the same strand is possible. This allows for a better understanding towards the development of real-time shape-changing DNA origami. The designed structures were folded to observe their ability to transform from one shape to the next, using strand displacement as proof of principle for the occurrence of shape-changes. Various characterization methods were used, including gel electrophoresis, dynamic light scattering (DLS), and atomic force microscopy (AFM) in order to obtain information on the size and shape of the folded structures to confirm whether they folded appropriately and whether shape-change occurred.

CHAPTER ONE: INTRODUCTION

SECTION ONE

Interest in DNA origami nanoparticles has been growing significantly in recent years due to their versatility and potential uses. In 2006, Paul Rothemund published findings on the self-assembly of DNA molecules into specific predetermined shapes in a single step, laying down the DNA origami technique principles [1]. They contain two kinds of single stranded DNA molecules, a long scaffold strand and multiple short oligonucleotides called staple strands. This technique has since been further developed to create more complex shapes in 1, 2, and 3D [2] and applied for specific purposes, such as vaccine delivery [3], drug delivery [4], biosensing, and imaging [5, 6]. However, while the complexities of DNA origami have continued to increase and be researched to match specific applications, little is known on designing a shape-changing nanoparticle in real-time [7]. Such a nanoparticle would change how nanocarriers are used for drug delivery methods and increase their applications by expanding their targeting and release capabilities by making them more specific and sensitive to their environment. Because DNA origami nanoparticles can self-assemble, it is hypothesized that simultaneously folding the same scaffold strand with staple strands for two different structures will produce both shapes and they will be able to shift back and forth between each other using different type of actuatable crosslinking methods, including pH change,

temperature change, and strand displacement. Each method will have different efficiency and will require different times for actuation.

SECTION TWO

DNA origami is a relatively new, yet fast-growing research field that has started in the early 2000's. Although it is quite young, a vast amount of development and work has been put into it due to its unique capabilities [1]. DNA origami is the art of folding DNA molecules into nanostructures with prescribed shapes and sizes that may be used as nanocarriers for various biological applications such as drug and vaccine delivery. What sets the DNA origami method separate from other methods of developing nanostructures is its biocompatibility as well as its ability to be used to fabricate nanoscale constructs that are difficult to obtain through other approaches such as inorganic, lipid-based, and polymeric nanoparticles [8]. This has allowed for researchers to develop arbitrarily shaped complex 3-dimensional nanostructures that had been previously impossible to obtain with an unprecedented structural fidelity [9].

One possibility that arises from the use of DNA origami is producing real-time shape-changing nanostructures [10]. Indeed, the DNA molecule is a versatile material that can be modified and assembled in various motifs that can react with the biological environment without producing toxic effects [11]. For instance, DNA motifs such as G-quadruplex or I-motifs are extremely sensitive to the pH or aptamers (that are short ssDNA with specific secondary structures) can change their structure upon binding biomolecules [12]. Because of this, DNA origami may be the optimal method to develop

a real-time shape-changing nanostructure. Having such a nanostructure would allow for the development of newer, more advanced, and more efficient methods of drug delivery by creating actuatable nanocarriers that will release their cargo only in the presence of specific cells or biological conditions or better interact with cells at a given time by changing their surface of contact. For example, this type of structure could be used to trigger specific biological mechanisms by releasing or presenting biomolecules upon specific stimuli such as a change in pH, presence of specific biomolecules (e.g., RNA or cytokines), or a change in temperature by 10°C. In addition, these nanostructures could revolutionize our way to design materials for regenerative medicine as it would pave the way to truly adaptable materials that will match the properties of living tissues.

Additionally, it has been noted that the shape of nanoparticles impacts their efficiency. For example, having an oblate shape has been seen to allow the nanoparticles to remain undetected by macrophages for a longer period of time [13]. This would allow for the nanoparticle to remain in the bloodstream for longer, providing more opportunity for it to reach the targeting site. Additionally oblong nanoparticles seem to have greater targeting avidity than nanospheres [13]. The shape of the nanoparticle has an impact on its interactions with cell membrane. It has been found that larger DNA nanoparticles with a greater compactness are more likely to allow for cellular internalization to take place rather than elongated, high-aspect-ratio nanoparticles [14]. Additionally, cellular uptake has been seen to be affected by cell–particle adhesion, strain energy of the membrane surrounding the nanoparticle, and local nanoparticle concentration at the cellular membrane. All of these factors are dependent upon the shape of the nanoparticle [15]. As

such, it is apparent that the shape of nanoparticles has an impact on their functionality, and as such is an important topic to note [16].

CHAPTER TWO

SECTION 1: DNA ORIGAMI FOLDING PROCESS

DNA origami structures are assembled with two different types of single stranded DNA strands [17]. The first is a long single-stranded DNA called the scaffold strand. In any DNA origami structure, there is only one scaffold strand that runs through the entirety of the structure, acting as a backbone. The second type of DNA strand is the short oligonucleotides, known as the staple strands [18]. There are several of these contained within a singular structure, and they are named as such due to the fact that they "staple" the scaffold strand into the desired shape by crosslinking distant sections. There is an excess of these staple strands, and they are designed to have complimentary bases to different segments of the scaffold strand in such a manner that they bind appropriately to fold the prescribed shape [18]. **Figure 1** below from *Heck et. al*. demonstrates this folding process [19].

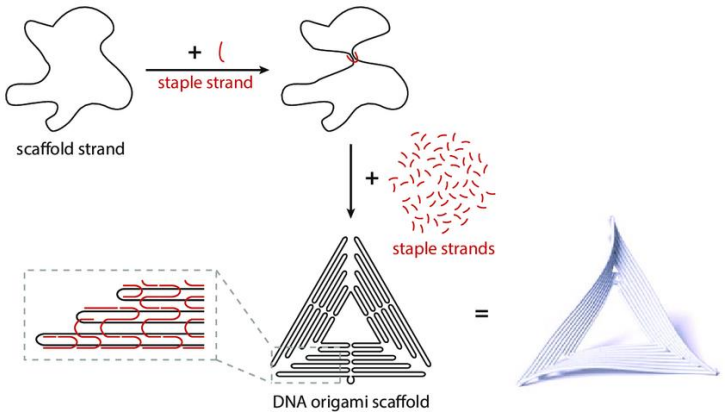

Figure 1. DNA Origami Folding Process

The DNA origami process of folding scaffold and staple strands together to form a triangle. The staple strands bind to various sections of the scaffold strand based on their nucleotide sequence, guiding the scaffold into the designated structure. [19]

Using the process of DNA origami, there have been a few steps towards developing a shape-changing nanostructure. For example, Torelli et al [20] developed a prototype nanorobot which is controlled by nucleic acid hybridization. This cylindrical nanorobot contains a switchable flap that reacts to an external stimulus and can switch from a disarmed to an armed position. The mechanism that opens the flap is operated through DNA coiling and is similar to a molecular spring. However, this method still requires more development as the flap is still unable to switch back from an armed position to a disarmed one. This is different from the shape-changing nanostructures that will be developed for this project. They will follow a cycle of shape-changes rather than an open versus closed state, which will allow for shape-changes to be more easily reversible. Additionally, there will be an ease of synthesis in this method because the nanostructures will be folded simultaneously.

Subsection 1: Scaffold Production

Prior to the folding of the DNA nanostructures, the appropriate scaffold must first be synthesized. This can be done through Polymerase Chain Reaction (PCR) based processes, or by using commercially available ssDNA such as M13mp18 [21]. The process that will be used here is called asymmetric Polymerase Chain Reaction (aPCR), which allows for the direct synthesis of ssDNA from any dsDNA, or ssDNA template [22]. This method also allows for exquisite control over the length and the sequence of the scaffold strands synthetized, which is critical to fold multiple structures on the same scaffold [23, 24]. In this process, an asymmetric concentration of primers is used to amplify a specific template, which is the desired scaffold strand. The limiting primer amplifies the complimentary strand and is used to generate a secondary template of the correct length [21]. A higher concentration of the abundant primer is then used to amplify the single strand of interest, the scaffold strand [21]. There are four steps in aPCR: Initial Denaturation, Denaturation, Annealing, and Extension, as well as a temperature hold at the end in order to maintain a proper temperature for storing the scaffold [25]. This process requires only a single reaction and will produce both the ssDNA of interest, as well as a small amount of dsDNA, which can be seen in **Figure 2** below [21].

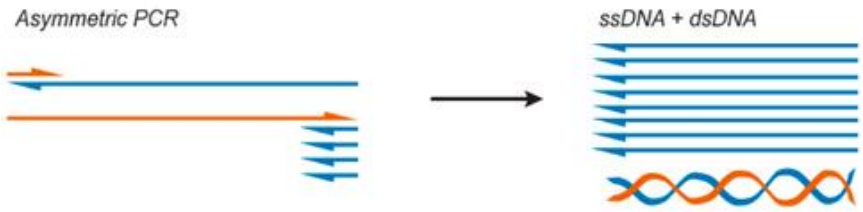

Figure 2. aPCR
The aPCR process with an asymmetric concentration of primers, resulting in the production of ssDNA and dsDNA [21]

Because this process in scaffold production also results in dsDNA, a purification step must be used prior to the folding of the nanostructures [26]. A method of purification used is to run gel electrophoreses using a low-melt agarose gel at 90 – 100 V for about 30 minutes. After running the gel, the ssDNA and dsDNA, along with other impurities will be apparent, and the ssDNA may be extracted. The purification process is continued using a gel extraction purification kit to dissolve the agarose containing the ssDNA, and centrifugation is performed in order to isolate the ssDNA from the agarose. After completing this process, the scaffold strand is purified through gel purification and is ready for folding.

Our preliminary results show in Figure 3 below a typical result for the production of a 2,298 bp scaffold strand in an agarose gel prior to purification that was generated for the structure that will be folded in this project. This result demonstrates my capability to perform aPCR and to generate enough scaffold for folding DNA origami structures.

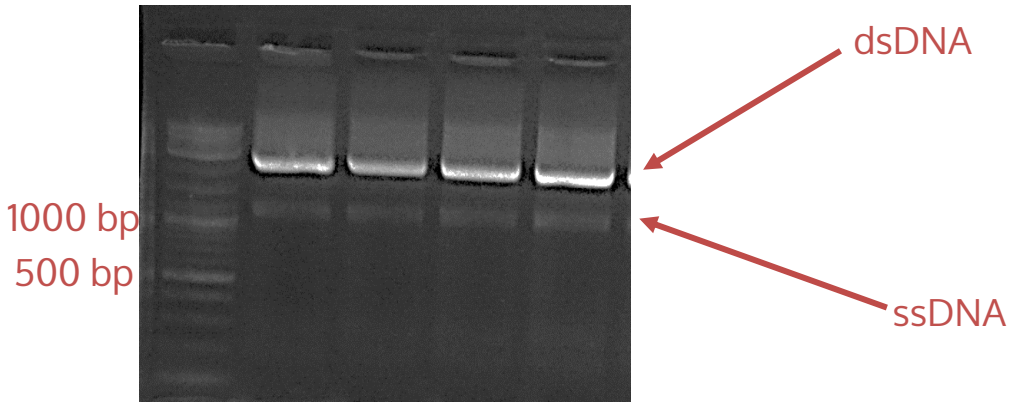

Figure 3. Low-Melt Gel
Shape-changing scaffold strand ran in 1.2% agarose gel after aPCR, prior to purification. The left column is the 1 kb ladder used for measuring molecular weight. Expected length and of the ssDNA was 2,298 bp.

The purified scaffold is combined with a mix of all staple strands in excess (10 to 20x molar ratio), as well as folding buffer ($MgCl_2$ + TAE) and placed within a thermocycler for folding, annealing from 90°C to 4°C overnight [27]. At the end of the folding period, the desired structures are produced, but will still need to go through a purification process with centrifugation to filter the excess staples [27].

SECTION 2: CHARACTERIZATION METHODS

Different characterization methods are required in order to determine the shape of a folded DNA origami nanostructure [28]. One method is known as Fluorescence resonance energy transfer (FRET) [29]. This is a type of energy transfer that occurs between two fluorophores in close enough proximity [29]. A donor fluorophore will absorb photons and jump from the ground energy state to the excited state, emitting a specific wavelength and transferring energy to the acceptor fluorophore [30]. This can be

visualized in **Figure 4** below. The acceptor fluorophore will then become excited and emit fluorescence if there is a spectral overlap between the acceptor excitation and donor emission [31]. Additionally, the two fluorophores must be within a 10 nm distance [29]. This method allows for the distance between two fluorophores to be determined based on the efficiency of the fluorescence, which will in turn allow for the determination of the distance between the sites the fluorophores are located on [29].

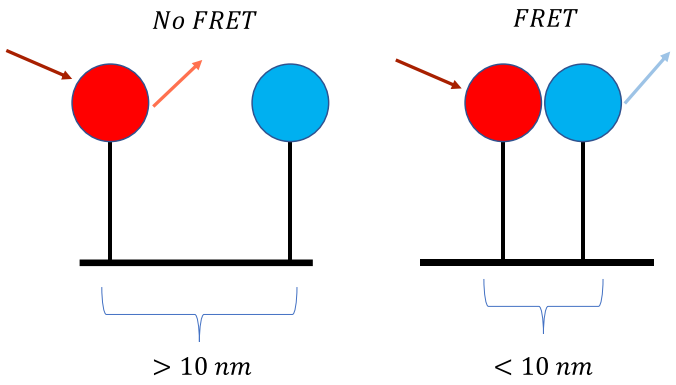

Figure 4. FRET
Schematic of FRET pairs. They must be located within 10 nm in order to produce FRET.

CHAPTER THREE: DESIGN AND FOLDING

The researched work is focused on establishing a real-time shape-changing DNA origami nanostructure. It is hypothesized that simultaneously folding the same scaffold strand with staple strands of two different structures will produce both shapes and they will be able to shift back and forth between each other via different actuation mechanisms. The main focus has been to develop a design that is possible to change into multiple shapes, as that has been noted to be the largest hurdle in the research [32]. There are two specific aims to this project. The first aim is to design the shape-changing nanostructures, including all shapes that will be developed. This includes the Triangle and Crescent, as well as the Tetrahedron. The second aim is the validation of the shape-change using strand displacement methods. This will include various characterizations of the nanoparticles, including AFM and DLS.

SECTION 1: SPECIFIC AIM 1

Specific Aim 1. Designing and characterizing shape changing DNA origami nanostructures.

The first aim of this project is to develop the designs of the shape-changing nanostructures, produce the scaffold and fold them.

Subsection 1: Designing the Structures

In order to begin developing a design, a tetrahedron from Veneziano et al [9] was uploaded to DAEDALUS to generate sequences and information on the format, including edge length, staple crossovers, and scaffold crossovers. After generating this design, the

tetrahedron was created in TIAMAT to help with modifications. This structure is pictured in **Figure 5** below as a PDB file in Chimera. Chimera is a program that allows for the interactive visualization and analysis of molecular structures [33]. The PDB file was generated by taking the TIAMAT file and uploading it to the TacoxDNA webserver, converting it to an oxDNA format, which was then converted into the PDB file to be viewed through Chimera [34]. The scaffold length of the Tetrahedron is 504 bases, and the structure contains 10 staple strands. The tetrahedron is not meant to change shape. Rather, it is meant to serve as a building-block for the shape-changing nanostructure, allowing for a more cohesive build and transition between each nanoparticle. By taking three copies of the same tetrahedron and rearranging them in various positions, different shapes can be achieved without drastic changes being necessary (**Figure 6 and Figure 7**).

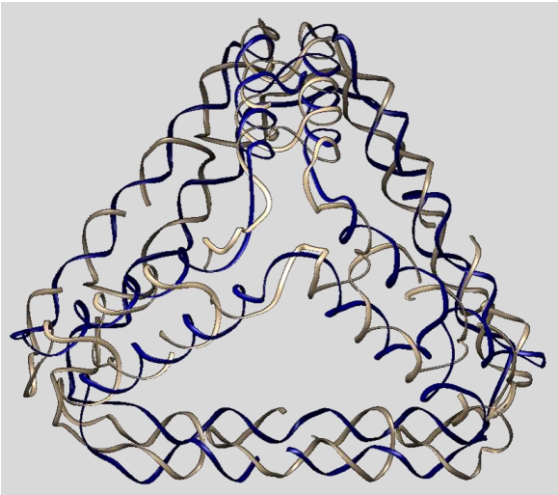

Figure 5. Tetrahedron
Designed tetrahedron pictured in Chimera. The scaffold strand is in blue and the 10 staple strands in beige [33].

After finalizing the Tetrahedron structure, the Triangle and Crescent structures were also designed in TIAMAT. Three copies of the tetrahedron are arranged in a particle orientation and connected together to form the first shape of the shape-changing nanostructure. This shape, pictured in **Figure 6** below, is called the Triangle due to its triangular organization. The second shape of the shape-changing structure is formed in a similar manner, connecting three copies of the same tetrahedron together, but in a different orientation, producing a shape called the Crescent pictured in **Figure 7** below.

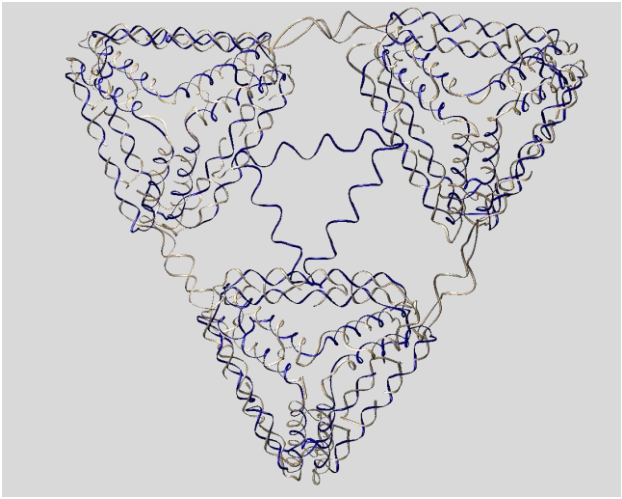

Figure 6. Triangle
Designed Triangle pictured in Chimera. The scaffold strand is in blue and staple strands in beige [33].

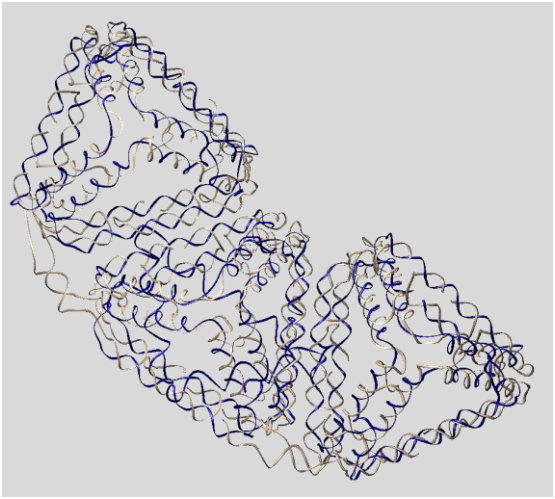

Figure 7. Crescent
Designed Crescent pictured in Chimera. The scaffold strand is in blue and staple strands in beige [33].

Both the Triangle and Crescent have the same scaffold strand, containing the same sequence of 1,632 bases. Additionally, they share 25 staple strands. The Crescent

contains its own specific seven staple strands, while the Triangle has eight. This minor difference in staple strands is due to using the tetrahedron as the bases for both structures. This method of designing appears to have allowed different shapes to be constructed from the same scaffold strand while keeping a majority of the staple strands. Using the tetrahedron as a building block allows for the general backbone of the structure to remain the same, only requiring these designated sections of the nanostructure to shift in order to produce the different shapes.

The Triangle and Crescent structures are not composed of just free-flowing tetrahedrons connected solely through the scaffold strand. They are cohesive and have their own stable shapes, supported by variously located staple strands at the adjacent vertices between tetrahedrons. In comparison, there were two more designs made by just adding more tetrahedrons onto the same scaffold strand, without incorporating additional staple strands. The first design can be seen in **Figure 8** where two tetrahedrons are connected only by the scaffold strand. This shape is referred to as 2Tet. The second design is seen in **Figure 9** where 3 tetrahedrons are joined through the scaffold strand and is referred to as 3Tet. These structures are amenable to be transformed into various shapes and it is easy to increase the number of tetrahedron on one scaffold to increase the complexity of the final assembly.

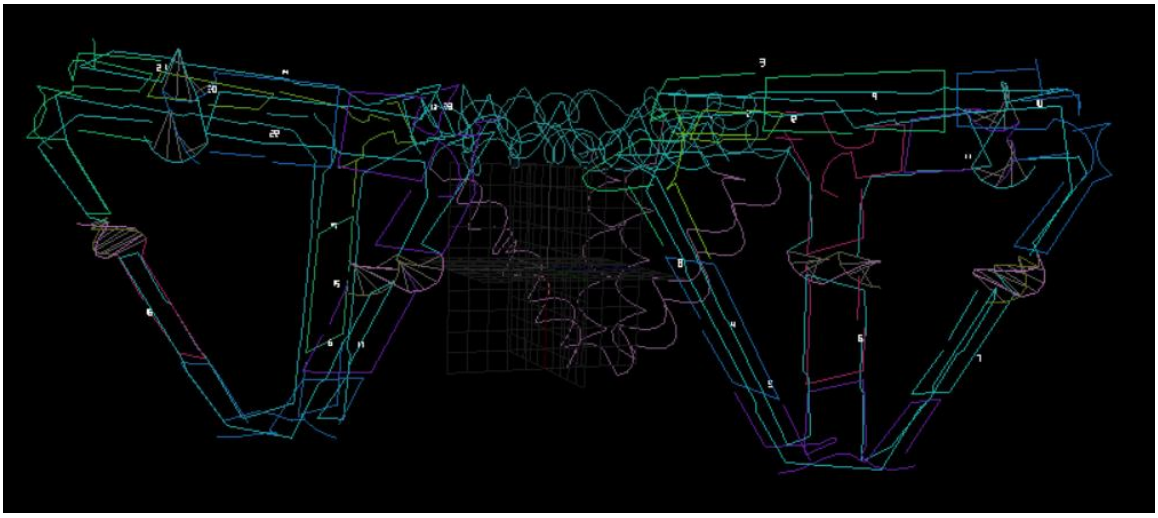

Figure 8. 2Tet
Designed 2Tet pictured in TIAMAT.

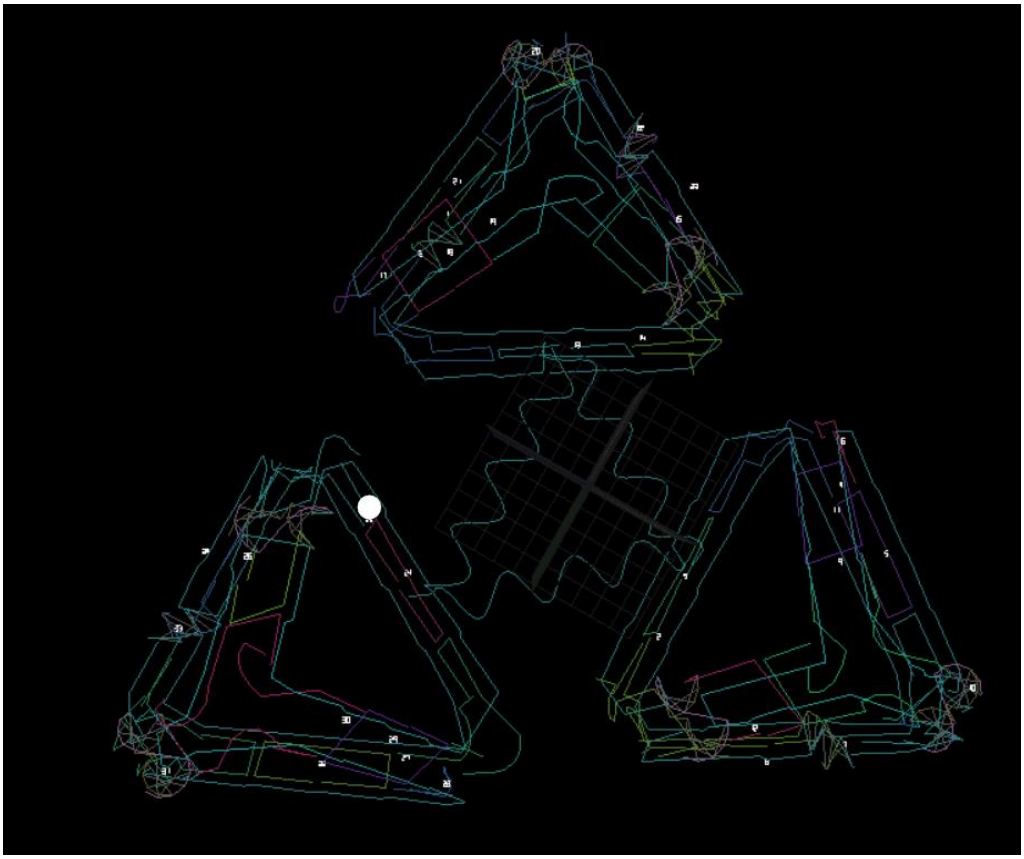

Figure 9. 3Tet
Designed 3Tet pictured in TIAMAT.

The last structure designed is called the Pyramid. This structure was designed by adding a fourth tetrahedron to the Triangle shape at the top of all three peaks, producing a pyramid-like shape. This structure has a longer scaffold strand than all previous structures, with 2306 bases, and is the only structure that will not be folded. This design demonstrates that various other shape-changing structures can be designed with additional tetrahedrons, opening various other possibilities for shape-changing structures. **Figure 10** below depicts the Pyramid in TIAMAT.

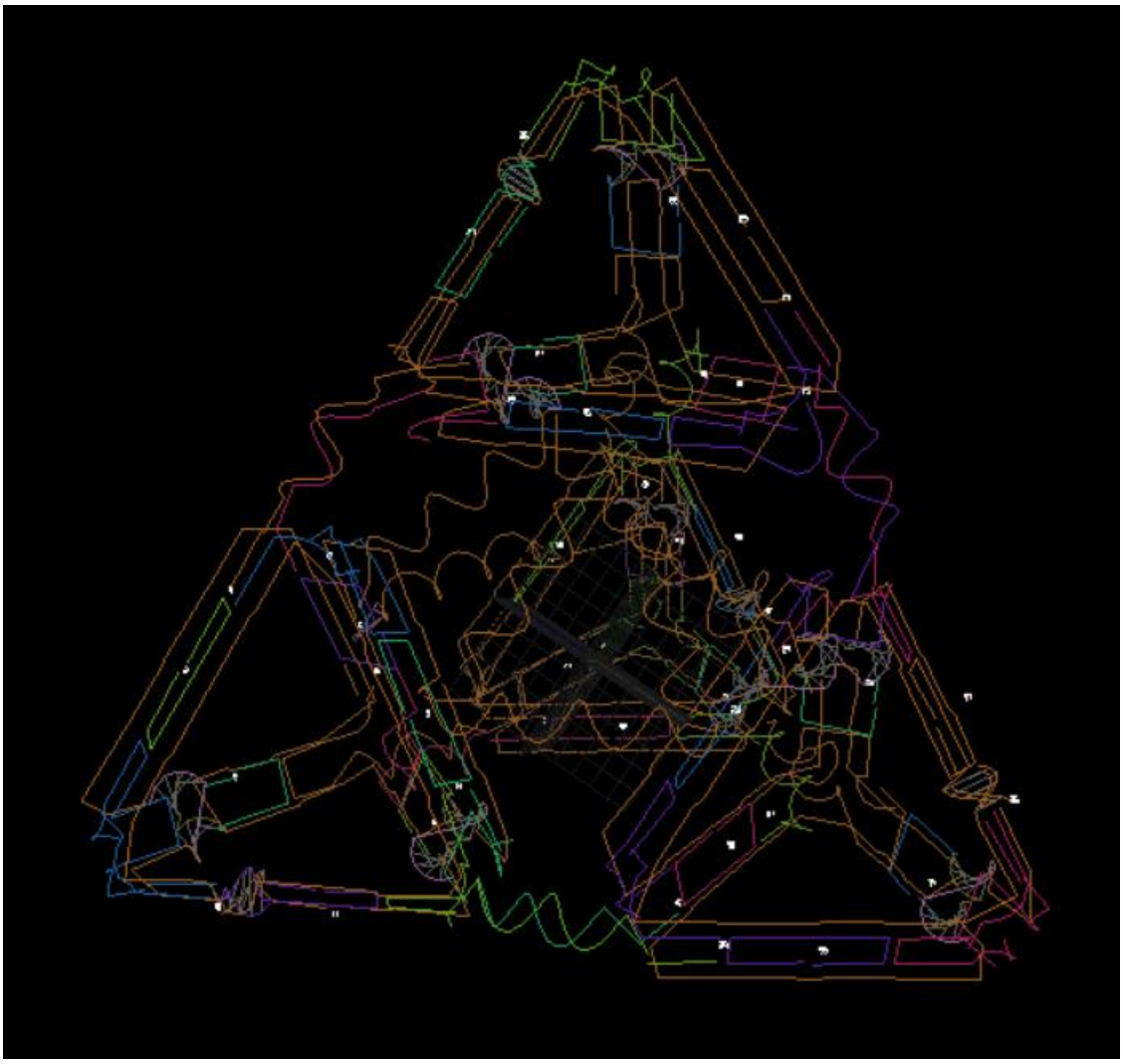

Figure 10. Pyramid
Designed Pyramid pictured in TIAMAT.

Subsection 2: Scaffold Production via aPCR

In order to demonstrate that the various shapes can be produced and change shape in real-time, various experiments must be conducted. As such the nanostructures must be folded, requiring the shape-changing scaffold to be synthesized. This is done through the same aPCR process explained in the **Background knowledge** section. Both an enzyme

called OneTaq, as well as LongAmp Taq polymerase were used for this production. It was found that scaffold produced with the OneTaq Enzyme had an average concentration of 281 nM, while scaffold produced with the LongAmp Taq polymerase had an average concentration of 602 nM. All three structures, the Tetrahedron, Crescent, and Triangle, are folded on the same scaffold strand, so only one method of production will be used. Because the tetrahedron is much smaller, its staple strands will only fold with the sections of the scaffold strand that are necessary for the nanoparticle. The specific settings within the thermocycler for the production of the shape-changing scaffold are shown in **Table 1** below. These settings take into account multiple factors including the size of the scaffold [35].

Table 1. *Specifications for aPCR process of shape-changing scaffold*

Step	**Temperature**	**Time**	
Initial Denaturation	94 °C	60 seconds	
Denaturation	94°C	20 seconds	30 cycles
Annealing	55°C	30 seconds	
Extension	68°C	3 minutes	
Temperature Hold	4°C	∞	

In addition to the scaffold production, various staple mixes must be made. For this project, six different mixes will be used. The first is the staple mix for the Tetrahedron.

Due to the low number of staples, it will have a very high concentration and will require to be diluted down to a concentration of 12.5 µM. The second staple mix is for the Crescent and will have a concentration of 15.625 µM. The third staple mix is for the Triangle and will have a concentration of 15.1515 µM. The fourth staple mix will be for both the Triangle and Crescent together, for experiments specific to noting real-time shape-changes. This staple mix will have a concentration of 12.5 µM. The fifth staple mix is for the 2Tet structure. Like the Tetrahedron, this staple mix will also need to be diluted down to a concentration of 12.5 µM. Lastly, the sixth staple mix is for the 3Tet structure and will have a concentration of 15.151 µM. The sequences for the scaffold strands and all staple strands can be seen in the **Appendix** section.

Subsection 3: Folding of the Nanostructures

The folding for all nanostructures will have a concentration of 30 µM of the scaffold and 300 µM of the staples. They will be made for 50 µL volume samples, with 5 µL of 10X Folding Buffer (FB), and water to reach the full volume. After folding in the thermocycler, all samples are purified through centrifugation to filter the excess staples and are run along with the scaffold in a high-melt agarose gel. **Figure 11** below shows the Tetrahedron, Crescent, and Triangle run on an agarose gel together. It can be seen that all folded samples are located higher in the gel than the scaffold, showing that they did indeed fold [36]. Additionally, a sample containing both the Crescent and Triangle shape folded together is also shown, and a difference in molecular weight from other folded samples can be seen. Additionally, **Figure 12** shows the Tetrahedron, 2Tet, and 3Tet

structures run on an agarose gel, and a difference in molecular weight can be seen between them, with the Tetrahedron being smaller.

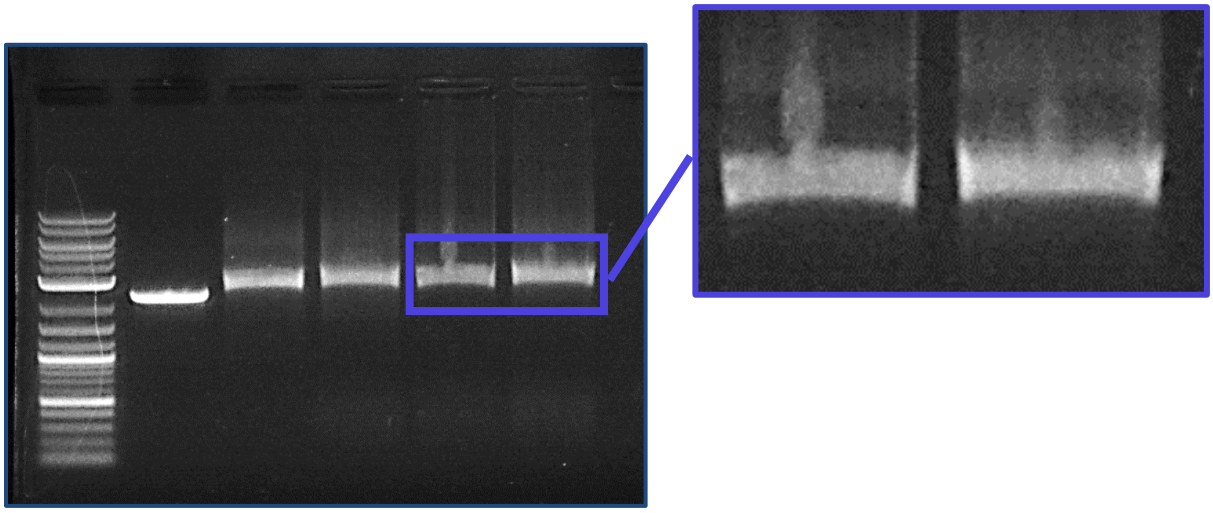

Figure 11. High-Melt Gel 1

0.7% High-melt gel. From left to right: Ladder, shape-changing Scaffold, Tetrahedron, Crescent, Triangle, Crescent & Triangle folded in same sample. Boxed image shows comparison between Triangle sample and Crescent & Triangle folded in same sample. A small difference in molecular weight is noted.

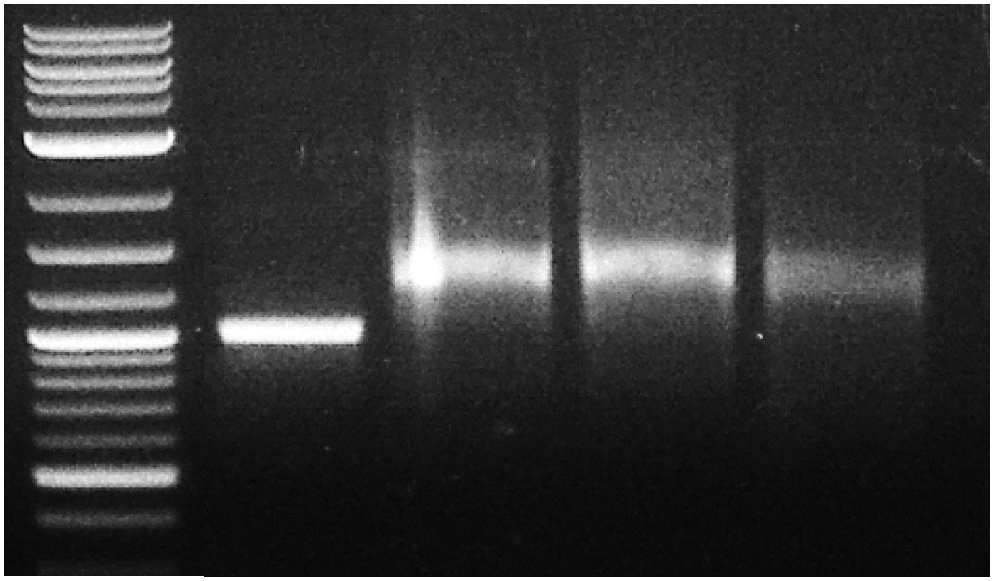

Figure 12. High-Melt Gel 2

0.8% High-melt gel. From left to right: Ladder, shape-changing scaffold, 2Tet, 3Tet, Tetrahedron. A difference in molecular weight is noted, with the Tetrahedron being smaller.

CHAPTER FOUR: VALIDATION OF SHAPE-CHANGE

As previously mentioned, there are two specific aims to this project. After covering the first aim and establishing the designs and folding of the various structures, the second aspect of this research will aim to further establish shape changing. The second aim is the validation of the shape-change using strand displacement methods. This will include various characterizations of the nanoparticles, including AFM and DLS.

SECTION 1: SPECIFIC AIM 2

Specific aim 2. Validating the actuation of the shape changing DNA origami.

The second aim of this project is to validate the shape-change of the nanostructures in real-time using strand displacement.

Subsection 1: Stimuli for shape-changing

The structures folded in specific aim 1 were redesigned to include strands that can bridge multiple structures together and can be displaced to change the final assembly of multiple structures. Firstly, the Triangle structure was folded and purified through the previously mentioned method in **Chapter 3.1.3**. After doing so, the Crescent staple mix was added at 20 times the concentration of the scaffold, and the sample was left in the thermocycler for 10 hours at 37°C to produce a shape change from Triangle to Crescent through displacement. The sample was then purified through the same centrifugation process, and a gel was run containing the Triangle, Crescent, and shape-changed samples, depicted in **Figure 13** below. A shift can be seen within the gel between the Tri-to-Cres sample and the Triangle sample. However, the Tri-to-Cres sample is located at the same

position as the Crescent sample, showing that the Tri-to-Cres sample may have in fact changed from the Triangle shape to the Crescent shape.

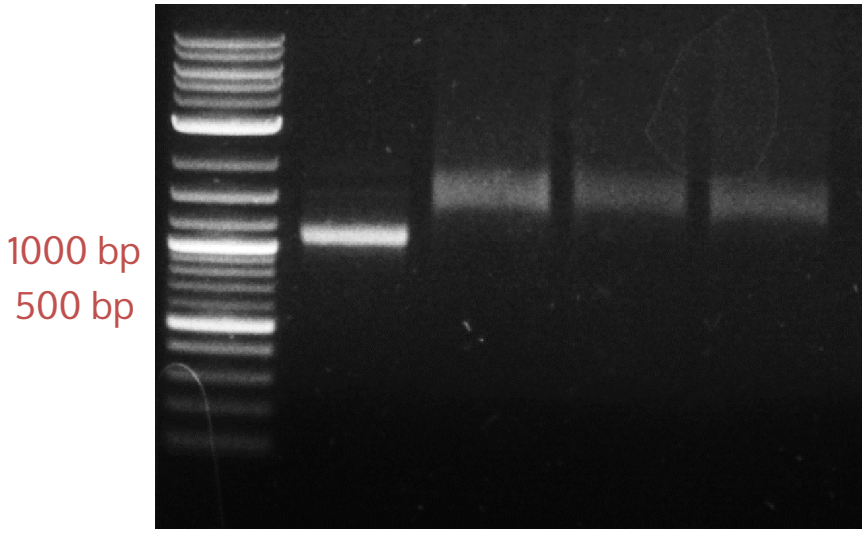

Figure 13. High-Melt Gel 3

0.8% High-melt agarose gel. From left to right: Ladder, shape-changing scaffold, Crescent, Tri-to-Cres, Triangle. A shift can be noted between the Triangle and Tri-to-Cres, with the Triangle appearing further down the gel and the Tri-to-Cres appearing at level with the Crescent.

Subsection 2: FRET System

While gel electrophoresis displays changes in molecular weight and allows for folded samples to be seen, it does not display the actual shape of the samples. A method for noting whether the desired structures have been achieved is necessary. One method that is used is FRET. The specific dyes that were used are FAM (donor) and TAMRA (acceptor), which can be easily attached to nucleic acids. Placing FRET pairs at specific locations within the structures provides necessary information about distances between

key locations of interest. Additionally, this will allow for testing the shape-changing capabilities between the Triangle and Crescent structures. Having FRET pairs at a location on the nanostructures that will change distance will allow for the florescence emission to provide information on which prescribed shape is present [30[37]].

The FRET experiments were conducted with the Tetrahedron and Crescent structures. First, two different samples were folded for each shape, one with only the donor fluorophore, and one with both the donor and acceptor fluorophores. The donor-only samples were to be used as a control. The folding process was the same as in other experiments, and the samples were purified through centrifugation. Afterwards, 40 µl of each sample at about 100 nM concentration was then placed into the fluorescence plate reader to observe the fluorescence. **Figures 14 and 15** below depict the graphs of fluorescence of each of the samples. In **Figure 14**, we see that the donor-only Tetrahedron sample does not produce FRET, but the donor-acceptor sample does. Because fluorescence is observed, we can determine the fluorophores are located within 10 nm of each other, meaning that the strands of their locations are in fact within 10 nm of each other. However, this is not observed with the FRET pairs on the Crescent structure. As seen in **Figure 15**, the donor-acceptor sample does not produce FRET, showing that the position of the fluorophores is not within 10 nm of each other, providing us with a clearer visualization of the structure.

The FRET efficiency (E) of the Tetrahedron structure was calculated by taking the fluorescent intensities of the donor-only Tetrahedron (I_D) and donor-acceptor Tetrahedron (I_{DA}) and subtracting them from each other. **Equation 1** below from Oktay et. al. was

used to find that the efficiency is about 34%, which is typical for this type of structure [24].

Equation 1

$$FRET\ efficiency\ (E) = \frac{I_D - I_{DA}}{I_D}$$

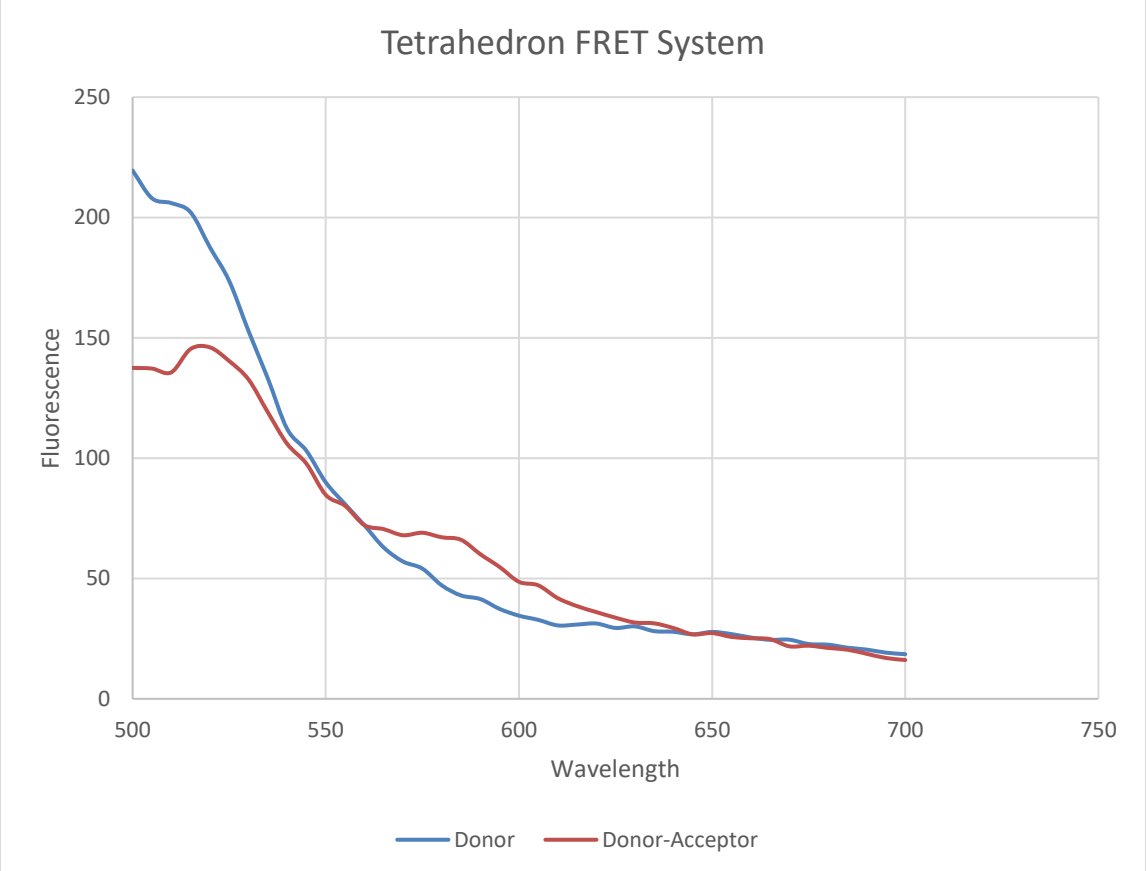

Figure 14. FRET of Tetrahedron

Graph of FRET on Tetrahedron structure. The blue line represents the Donor-only sample containing only FAM, and the orange line represents the Donor-Acceptor sample with both FAM and TAMRA. The Donor-Acceptor sample has a second lower peak at about 580 Wavelength, showing that there is FRET produced.

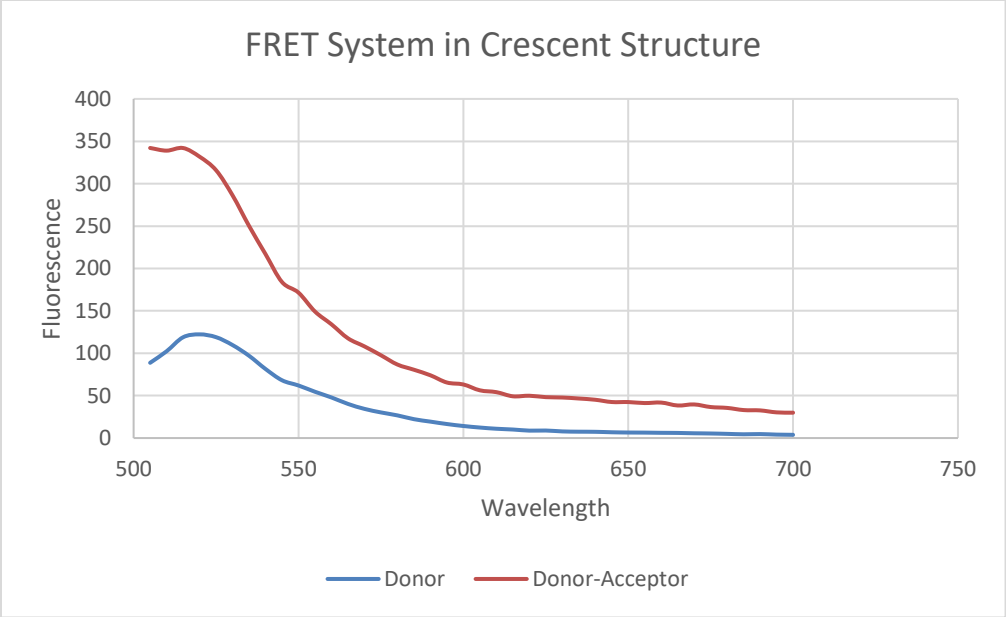

Figure 15. FRET of Crescent

Graph of FRET System in Crescent structure. The blue line represents the Donor-only sample containing only FAM, and the orange line represents the Donor-Acceptor sample with both FAM and TAMRA. FRET is not seen, there is a lack of a second peak in the Donor-Acceptor sample.

Subsection 3: AFM

Another test that has been conducted is Atomic Force Microscopy (AFM). AFM is a high-resolution scanning probe microscopy that allows for the visualization of our structures with nanoscale precision [38]. Obtaining images from AFM of all structures further demonstrates their correct folding of the structure and validates our models. Additionally, acquiring AFM images of a sample containing both the Crescent and Triangle folded together provides insight on which shape the scaffold is more inclined to fold into when folded concurrently. Furthermore, acquiring images of the samples produced with strand displacement will further demonstrate real-time shape-changing

capabilities of the nanostructures. **Figures 16 through 22** show all AFM images of various samples. It can be seen that all structures folded appropriately. Additionally, the Tri-to-Cres sample demonstrates the shape-changing capabilities of the nanostructure, with about 75% of the nanostructures either fully achieving the Crescent shape, or being in the process of changing into the Crescent shape.

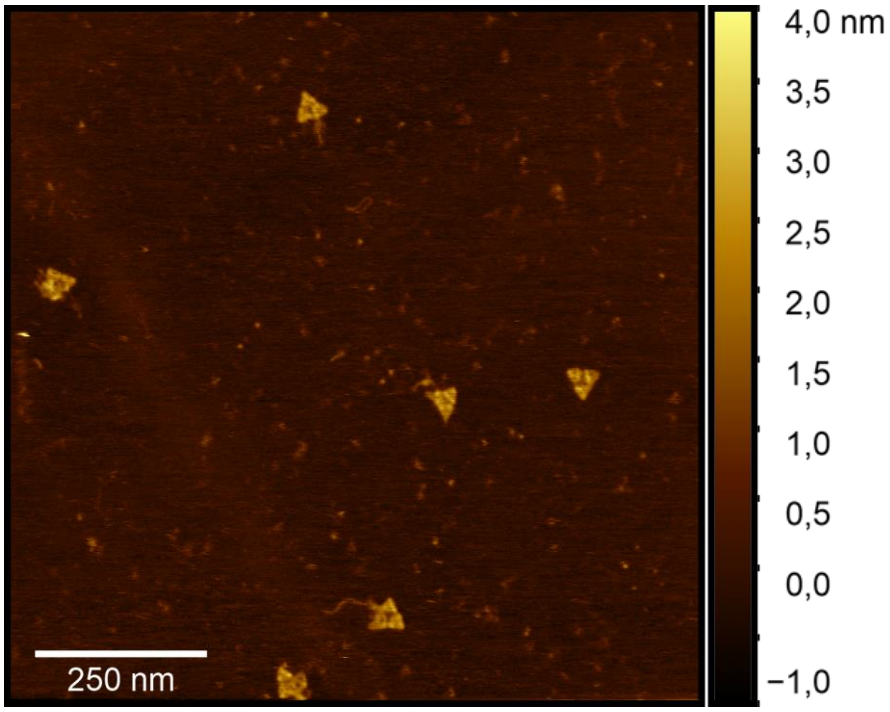

Figure 16. AFM of Triangle

AFM image of folded Triangle structure. The corners of the three connected Tetrahedrons can be seen in the appropriate arrangement.

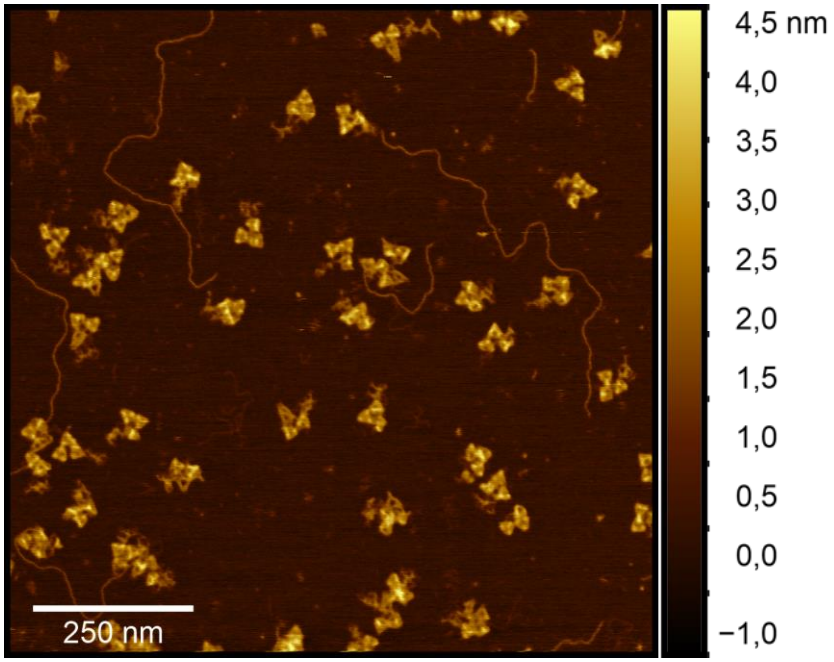

Figure 17. AFM of Crescent

AFM image of folded Crescent Structure. The connected tetrahedrons can be seen in the appropriate arrangement. Note that an opening can be seen between the two farthest tetrahedrons on the structure.

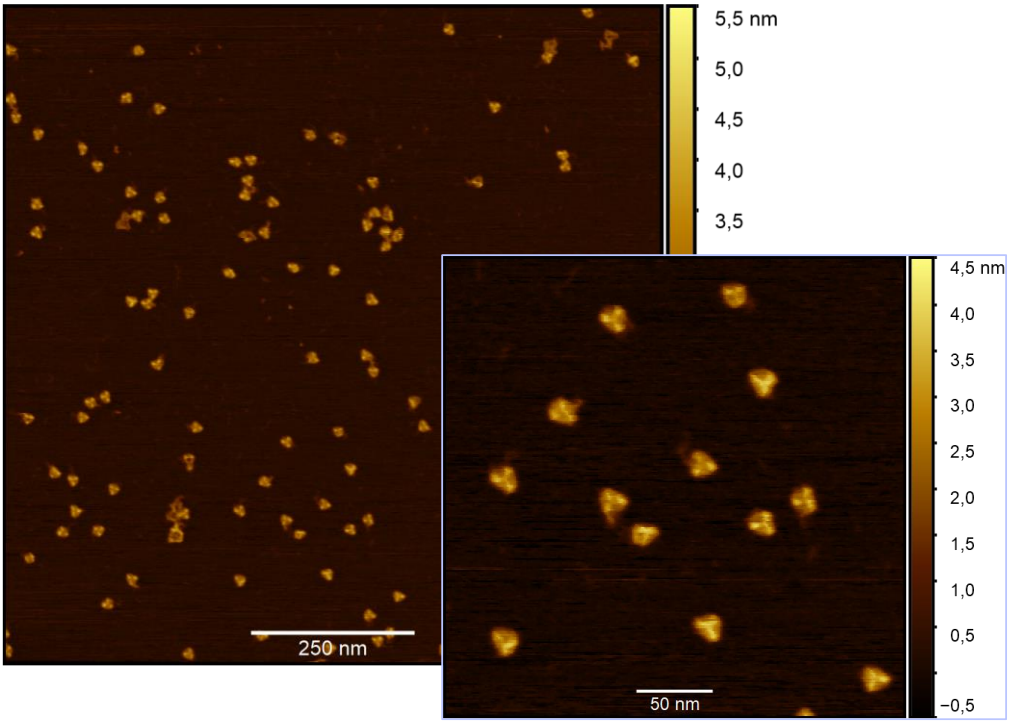

Figure 18. AFM of Tetrahedron

AFM image of folded Tetrahedron structure.

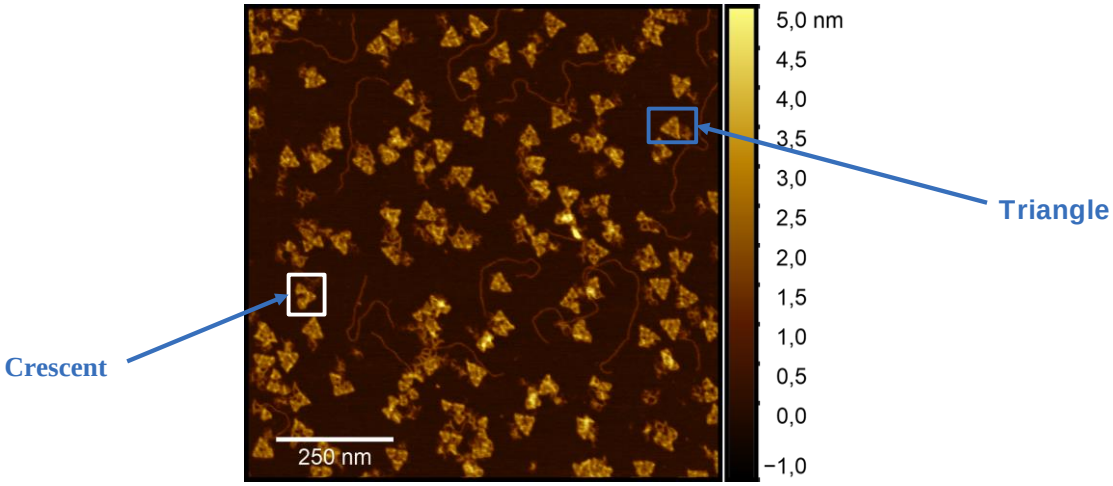

Figure 19. AFM of Tri-to-Cres

AFM image of folded Tri-to-Cres shift with strand displacement. Several Crescent structures can be seen, as well as some Triangles, demonstrating shape-change through strand displacement.

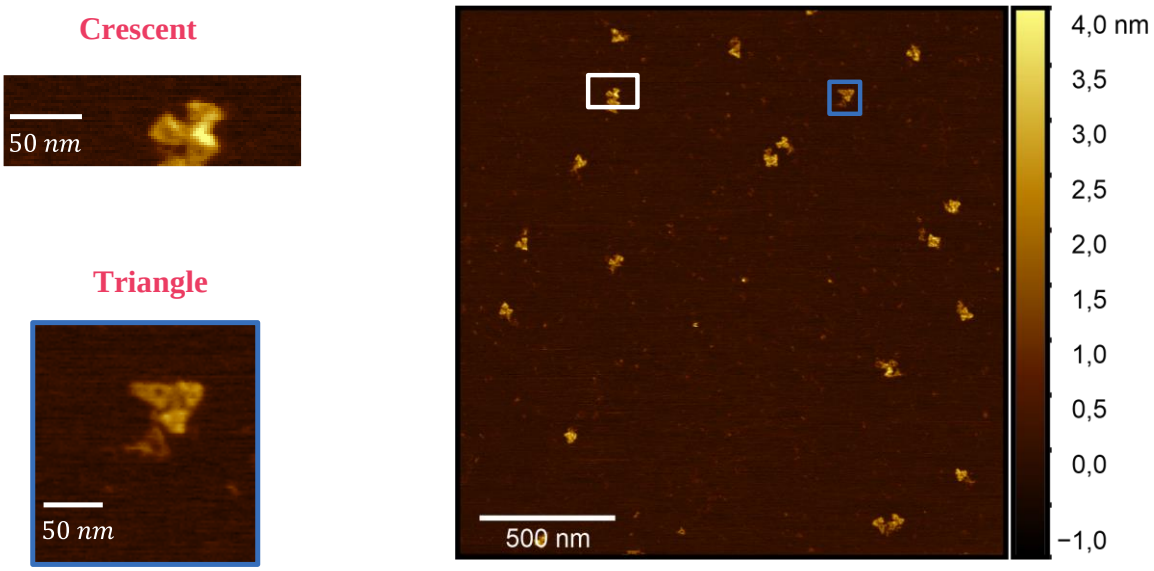

Figure 20. AFM of Crescent and Triangle

AFM image of both Crescent and Triangle folded structures. Both orientations can be seen.

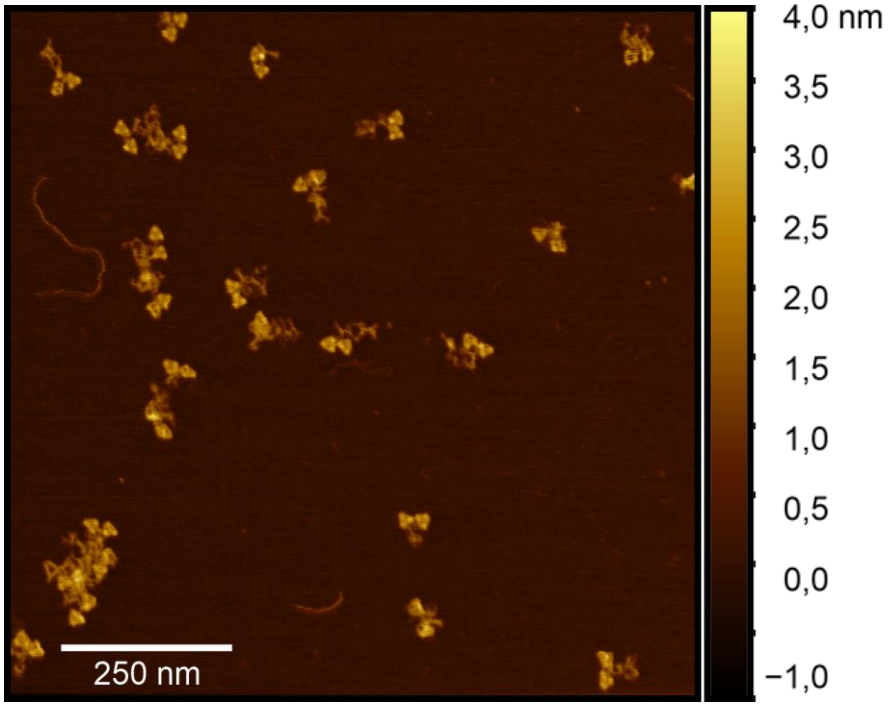

Figure 21. AFM of 2Tet

AFM image of 2Tet structure. Two tetrahedron figures can be seen along the scaffold strand.

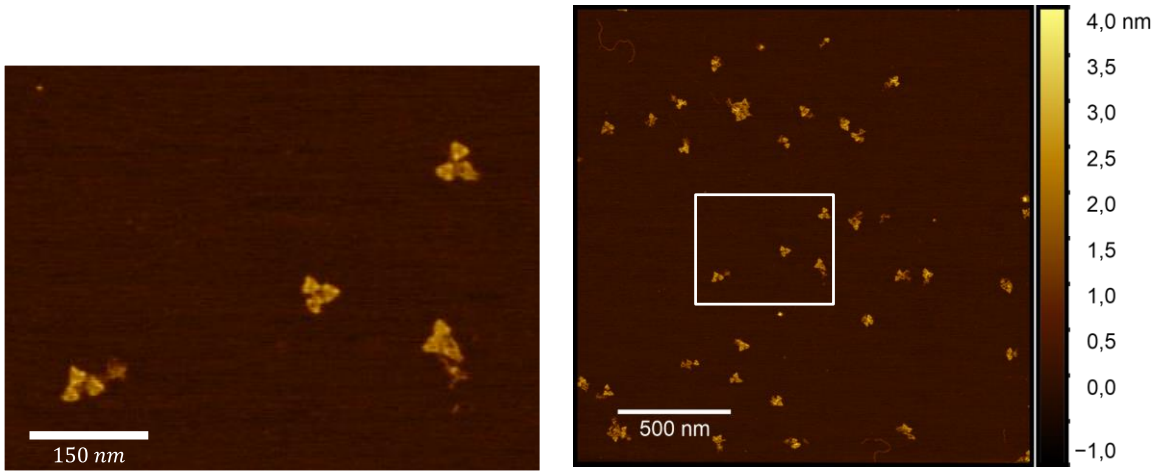

Figure 22. AFM of 3Tet

AFM image of 3Tet structure. Three tetrahedron figures can be seen along the scaffold strand.

Subsection 4: DLS

The last experiment conducted was with Dynamic Light Scattering (DLS). DLS allows for the size of nanoparticles to be measured by directing light at the sample and detecting the scattered light at a certain angle. DLS measurements were taken for the Tetrahedron, Triangle, Crescent, and Tri-to-Cres samples using 80 µl of each sample at a 20 nM concentration. Each sample was placed in both a 1X PBS solution and a 1X FB solution for the measurements. The results of these measurements can be seen in **Figure 23**, which shows the average measurement of each sample. Additionally, **Figure 24** shows mean intensity measurements in the DLS machine for each of the samples in 1X PBS, and **Figure 25** shows the samples in 1X FB. In **Figure 23**, we can see that the Crescent structure had the smallest average size in both the FB and PBS solutions. Of all samples in the FB, the Triangle had the largest size, followed by the Tetrahedron. However, in PBS the Tetrahedron was slightly larger than the Triangle. While the Tetrahedron does have a smaller size in the design, it is shown as being larger in the DLS measurements. This may be due to how the samples interact within the solutions. Because they are so small, the DLS instrument may instead be registering large groups of the nanostructure as one nanoparticle. They may also be more aggregated than the other samples. Additionally, the Tri-to-Cres sample had a smaller size than the Triangle in both FB and PBS and was closer in size to the Crescent sample. This shows that there was a change that occurred during the strand displacement process, causing the nanostructure to change size, which may be a result from a change in shape.

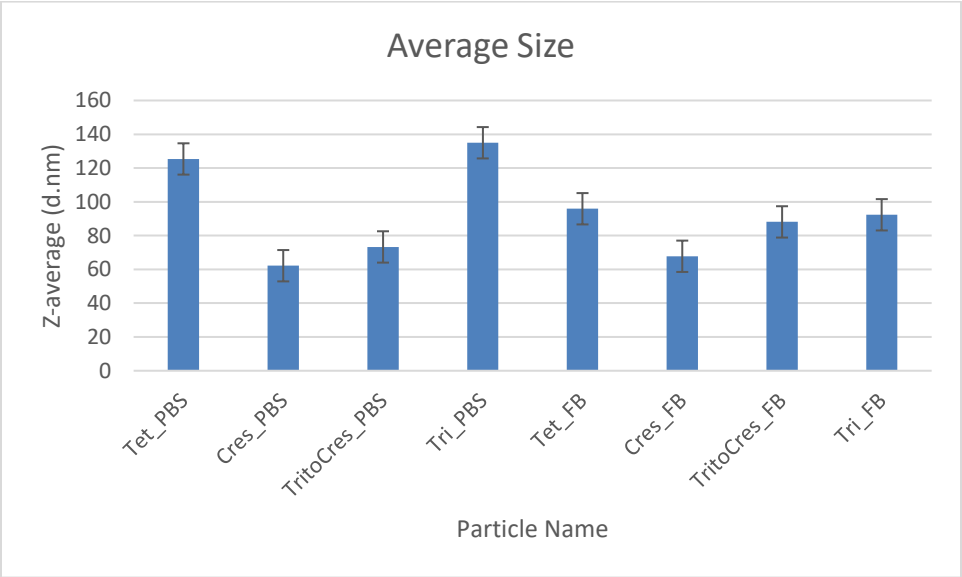

Figure 23. DLS Bar Graph

Bar graph of average size measurements from DLS machine of Tetrahedron (Tet), Crescent (Cres), Tri-to-Cres, and Triangle (Tri) in both 1X PBS and 1X FB.

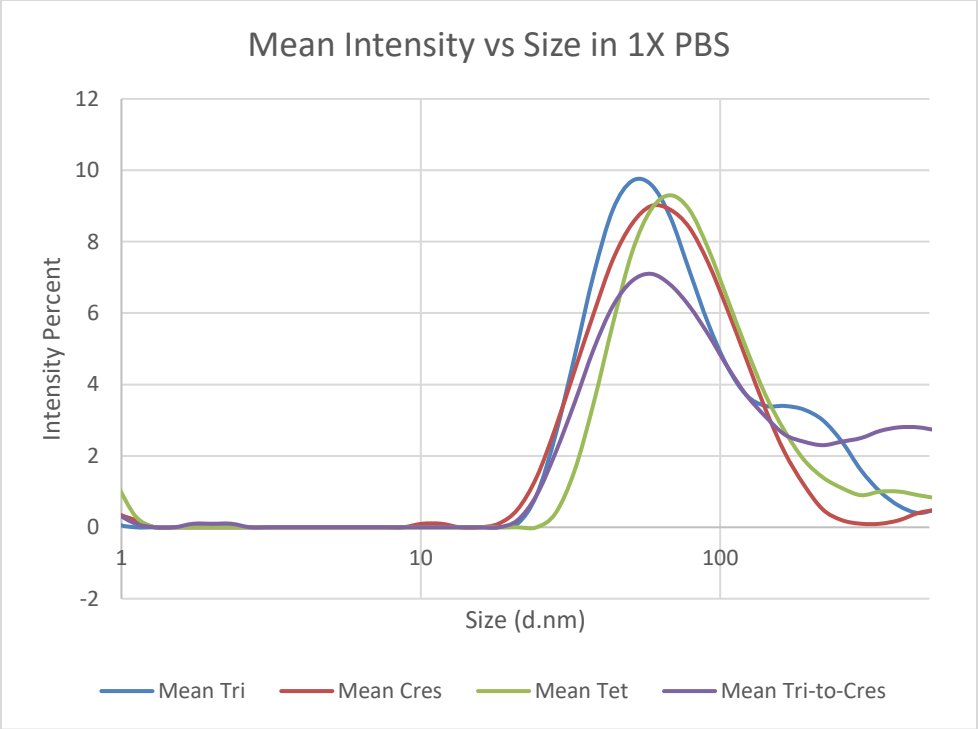

Figure 24. DLS Mean Intensity PBS

Mean intensity of each sample in 1X PBS. There is a shift between the Triangle and Tri-to-Cres samples.

Figure 25. DLS Mean Intensity FB

Mean intensity of each sample in 1X FB. There is a shift between the Triangle and Tri-to-Cres samples.

CHAPTER FIVE: CONCLUSIONS AND FUTURE WORK

The researched work focuses attention on three main things. The first is how to design several DNA origami shapes from the same scaffold strand. There has been a lack in the literature on developing such designs, and this is an important factor for developing shape-changing DNA origami. The second point of focus is folding such nanoparticles and ensuring that all nanostructures can in fact be produced. Lastly, this work aims to bridge the gap in the literature in real-time shape-changing nanostructures by establishing whether the designed nanoparticles can in fact change shape in real-time between both prescribed designs. Doing so is important in order to take a step towards advancing current methods of drug delivery.

The design aspect of the work was established, with a total of six nanostructures designed in TIAMAT. These structures are the Tetrahedron, Triangle, Crescent, 2Tet, 3Tet, and Pyramid. These designs demonstrate that it is possible to design multiple different structures with the same scaffold strand. The use of the Tetrahedron as a building block for all other structures significantly simplified the process, allowing for a smoother transition in the design changes. Additionally, having the 2Tet and 3Tet designs highlight how the connection between tetrahedrons are important for the development of specific shapes, rather than just producing free-flowing tetrahedrons. The Pyramid structure demonstrates the capability of developing further designs through similar methods with additional tetrahedrons.

All designed structures were folded and purified except the Pyramid. The same scaffold was used for the production, changing only the staple mixes to produce different structures. The folded structures were purified and run on agarose gel to observe whether a shift will occur, signifying the folding of the shapes. All shapes appeared higher on the gel than the scaffold, showing the folding capabilities. Additionally, some differences were noted between the folded structures on the gel, demonstrating a difference in shape. It was also noted during the scaffold production for the structures that LongAmp Taq polymerase produced higher concentrations than through the use of the OneTaq enzyme, allowing for a better production method.

Three different characterization methods were also conducted in order to observe the features and shape-changing capabilities of the nanostructures. The first method was done through the use of FRET pairs. The fluorescence was observed in Tetrahedron samples with both the donor and acceptor fluorophores, but FRET was not achievable with the Crescent structure. This provides us with an accurate measurement of distance between the locations on the nanostructures, as they must be less than 10 nm apart. The second characterization method used was AFM, providing images of seven different samples to observe their shapes. The samples that were imaged were the Tetrahedron, Triangle, Crescent, Tri-to-Cres, 2Tet, 3Tet, and the Triangle and Crescent folded together. It was found that all samples folded appropriately, and shape-change was achieved through strand displacement. The last characterization method used was DLS. Acquiring size measurements of the Tetrahedron, Triangle, Crescent, and Tri-to-Cres samples provided information on the behavior and possible shape within the samples.

Although the Tetrahedron is the smallest of all the structures, its measurements were quite large in comparison. However, this may be due to aggregation. Additionally, the Tri-to-Cres structure measured slightly larger than the Crescent, but smaller than the Triangle. This suggests that a shape-change did occur, producing Crescent structures from previous Triangle structures.

This work establishes the design and folding of real-time shape-changing DNA nanostructures. However, more methods can be experimented with to produce shape-changing qualities, such as the use of pH sensitive motifs. Additionally, the efficiency of the shape-change is yet to be determined. A question that is yet to be answered is what percentage of nanostructures can be expected to change shape at a time. Now that the capability of shape-changing has been developed, it is important to further perfect these methods for optimization in order to for them to advance our capabilities of personalized medicine and introduce a new method of drug delivery.

APPENDIX

***Table 2**. List of all staple strands for all designed nanostructures:*

Triangle Staple	GAGCCACCACCAGGAGGTTGAGGACGGAATACACCGGAACCA
	CCATCTTTTCATTTTTTAATCAAAATAGTTTATTTTGTTTTTTCA CAATCAA
	AACCATCGATTAGCCCCCTTATTAGCGTTTGGTCACCAATGA
	TTTCATCGGCATTTTTTTTTCGGTCAAGCAGCACCGTTTTTTAAT CAGTAGCAGTTTGCCTTTTTTTTTAGCGTCAGAC
	CAGAGCCACGCCACCCTCAGAACCCGCGTTGTAGGCCACCCT
	CAGCGCTAAAGTTTTTACAAAAGGGCTATTGACGGAATTTTTA TTATTCATTCATTTGGGAATTTTTTTAGAGCCAGC
	ACTTGAGCAAAGGTGAATTATCACAATCAGACAGCGTCACCG
	TATGGTTTACAAAATCACCAGTAGCACCATTTAGAAAATTCA
	AAGGTAAAGACATTCAACCGATTGACCACGAACCAGGGAGGG
	TAAGCAGATAGTAGAAAATACATAATTTTCTTTTAAGAAAAG
	TTCACGTTAAAGGAATTGCGAATACCTTAAGACTATAATTTT
	TTCAGCGGAGTTTCTTAAACAGCTTGATACCCTTTCAACAGT
	TGAGAATAGAATTTTTAGGAACAACTGAAAATCTCCATTTTTAA AAAAAAGGTCAGCTTGCTTTTTTTTCGAGGTGAA
	TCGGTTTACTCCAAAAGGAGCCTTGCAGGGGCTTTAATTGTA
	CCCACGCATATCGGAACGAGGGTAGAGCAATAACAACCATCG
	CCTCAGCAGCGTTTTTAAAGACAGCAACCGATATATTTTTTTCG GTCGCTGAGAGTTAAAGGCTTTTTCGCTTTTGCG
	CGGAATACGAAACCGAGGAAACGCGTCACGGATCAATAATAA
	AGCCACCACCATAGTTAGCGTAATCTTCATTGCCACCCTCAG
	ATAAGTTTTGATGATACAGGAGTGCCTGTCAACGTACTGGTA
	TACCGTTCCATTCTGAAACATGAAAGTATTAGTCTCTGAATT
	GTAAGCGTCATTTTTTACATGGCTTTTAACGGGGTCATTTTTGT GCCTTGAGTGCCTATTTCGTTTTTGAACCTATTA
	ATGCCCCCTAACAGTGCCCGTATAGCCGTTAAGTAACAGTTA
	ATTAGCGGGGAGGTTTAGTACCGCCACCCTCGAAGGATTAGG
	AGGTGTATCACTTTTTCGTACTCAGGTTTTGCTCAGTTTTTTAC CAGGCGGACGAGAGGGTTGTTTTTATATAAGTAT
	ACACTGAGCCCAATAGGAACCCATGGAATAGCCCGTACCGTA
	CTCATTTTCAGTTTTTGGATAGCAAGTTTCGTCACCATTTTTTT TTTTTTTTTTTTTGGCCGGAAAC
	AGAACCGCCACTTTTTCCTCAGAACCAAAGCCAGAATTTTTTG GAAAGCGCA
	ACCATTAGCAATTTTTTTTTTTTTTTGTACAAACTAAGCATTCC ACATTTTTGACAACCCTC
	GCCGAACAAAGTTTTTTTACCAGAAGCCAAAAGAACTTTTTTT TTTTTTTTTTTTTTCTCCTCAAGA

	AGAGGCTGAGATTTTTTTTTTTTTTGGCATGATTATTACGCA GTATTTTTTGTTAGCAAAC
	AGCTATCTTACTTTTTCGAAGCCCTTGTATGGGGTTTTTTTTT GCTAAACAA
	GATAGTTGCGCTTTTTTTTTTTTTTTGCCGCCACCACAGAGCC GCCGTTTTTCCAGCATTGA
	CGGAACCGCCTTTTTTCCCTCAGAGCCCACCCTCAGATTTTTT TTTTTTTTTTTTTTCGACAATGAC
Crescent Staples	GAGCCACCACCAGGAGGTTGAGGACGGAATACACCGGAACCA
	CCATCTTTTCATTTTTTAATCAAAATAGTTTATTTTGTTTTTTCA CAATCAA
	AACCATCGATTAGCCCCCTTATTAGCGTTTGGTCACCAATGA
	TTTCATCGGCATTTTTTTTTCGGTCAAGCAGCACCGTTTTTTAAT CAGTAGCAGTTTGCCTTTTTTTTTAGCGTCAGAC
	CAGAGCCACGCCACCCTCAGAACCCGCGTTGTAGGCCACCCT
	CAGCGCTAAAGTTTTTACAAAAGGGCTATTGACGGAATTTTTAT TATTCATTCATTTGGGAATTTTTTTAGAGCCAGC
	ACTTGAGCAAAGGTGAATTATCACAATCAGACAGCGTCACCG
	TATGGTTTACAAAATCACCAGTAGCACCATTTAGAAAATTCA
	AAGGTAAAGACATTCAACCGATTGACCACGAACCAGGGAGGG
	TAAGCAGATAGTAGAAAATACATAATTTTCTTTTAAGAAAAG
	TTCACGTTAAAGGAATTGCGAATACCTTAAGACTATAATTTT
	TTCAGCGGAGTTTCTTAAACAGCTTGATACCCTTTCAACAGT
	TGAGAATAGAATTTTTAGGAACAACTGAAAATCTCCATTTTTAA AAAAAAGGTCAGCTTGCTTTTTTTTCGAGGTGAA
	TCGGTTTACTCCAAAAGGAGCCTTGCAGGGGCTTTAATTGTA
	CCCACGCATATCGGAACGAGGGTAGAGCAATAACAACCATCG
	CCTCAGCAGCGTTTTTAAAGACAGCAACCGATATATTTTTTTCG GTCGCTGAGAGTTAAAGGCTTTTTCGCTTTTGCG
	CGGAATACGAAACCGAGGAAACGCGTCACGGATCAATAATAA
	AGCCACCACCATAGTTAGCGTAATCTTCATTGCCACCCTCAG
	ATAAGTTTTGATGATACAGGAGTGCCTGTCAACGTACTGGTA
	TACCGTTCCATTCTGAAACATGAAAGTATTAGTCTCTGAATT
	GTAAGCGTCATTTTTTACATGGCTTTTAACGGGGTCATTTTTGTG CCTTGAGTGCCTATTTCGTTTTTGAACCTATTA
	ATGCCCCCTAACAGTGCCCGTATAGCCGTTAAGTAACAGTTA
	ATTAGCGGGGAGGTTTAGTACCGCCACCCTCGAAGGATTAGG
	AGGTGTATCACTTTTTCGTACTCAGGTTTTGCTCAGTTTTTTACC AGGCGGACGAGAGGGTTGTTTTTATATAAGTAT
	ACACTGAGCCCAATAGGAACCCATGGAATAGCCCGTACCGTA
	CAGAGCCGCCGTTTTTCCAGCATTGACGGAACCGCCTTTTTTCC CTCAGAGCCCACCCTCAGATTTTTGCCGCCACCA
	AGAACCGCCACTTTTTCCTCAGAACCAAAGCCAGAATTTTTTT TTTTTTTTTTTTTTGGCCGGAAAC

	ACCATTAGCAATTTTTTTTTTGGAAAGCGCAAGAGGCTGAGA TTTTTCTCCTCAAGA
	AGCATTCCACATTTTTTTTTTGGCATGATTATTACGCAGTATT TTTTGTTAGCAAAC
	GCCGAACAAAGTTTTTTTACCAGAAGCCAAAAGAACTTTTTT TTTTTTTTTTTTTTTGACAACCCTC
	AGCTATCTTACTTTTTCGAAGCCCTTGTATGGGGTTTTTTTTT GCTAAACAAGATAGTTGCGCTTTTTCGACAATGAC
	CTCATTTTCAGTTTTTGGATAGCAAGTTTCGTCACCATTTTTG TACAAACTA
3Tet Staples	GAGCCACCACCAGGAGGTTGAGGACGGAATACACCGGAACCA
	CCATCTTTTCATTTTTTAATCAAAATAGTTTATTTTGTTTTTTCA CAATCAA
	TATGGTTTACAAAATCACCAGTAGCACCATTTAGAAAATTCA
	CAGCGCTAAAGTTTTTACAAAAGGGCTATTGACGGAATTTTTTAT TATTCATTCATTTGGGAATTTTTTTAGAGCCAGC
	AAGGTAAAGACATTCAACCGATTGACCACGAACCAGGGAGGG
	ACTTGAGCAAAGGTGAATTATCACAATCAGACAGCGTCACCG
	ACCATTAGCAATTTTTGGCCGGAAAC
	AACCATCGATTAGCCCCCTTATTAGCGTTTGGTCACCAATGA
	TTTCATCGGCATTTTTTTTTTCGGTCAAGCAGCACCGTTTTTTTAAT CAGTAGCAGTTTGCCTTTTTTTTTAGCGTCAGAC
	CAGAGCCACGCCACCCTCAGAACCCGCGTTGTAGGCCACCCT
	CGGAACCGCCTTTTTTCCCTCAGAGCCCACCCTCAGATTTTTGC CGCCACCACAGAGCCGCCGTTTTTCCAGCATTGA
	AGCCACCACCATAGTTAGCGTAATCTTCATTGCCACCCTCAG
	AGAACCGCCACTTTTTCCTCAGAACCAAAGCCAGAATTTTTTG GAAAGCGCA
	TACCGTTCCATTCTGAAACATGAAAGTATTAGTCTCTGAATT
	GTAAGCGTCATTTTTTACATGGCTTTTAACGGGGTCATTTTTGT GCCTTGAGTGCCTATTTCGTTTTTGAACCTATTA
	ATAAGTTTTGATGATACAGGAGTGCCTGTCAACGTACTGGTA
	ATGCCCCCTAACAGTGCCCGTATAGCCGTTAAGTAACAGTTA
	AGAGGCTGAGATTTTTCTCCTCAAGA
	ATTAGCGGGGAGGTTTAGTACCGCCACCCTCGAAGGATTAGG
	AGGTGTATCACTTTTTCGTACTCAGGTTTTGCTCAGTTTTTTAC CAGGCGGACGAGAGGGTTGTTTTTATATAAGTAT
	ACACTGAGCCCAATAGGAACCCATGGAATAGCCCGTACCGTA
	CTCATTTTCAGTTTTTGGATAGCAAGTTTCGTCACCATTTTTGT ACAAACTAAGCATTCCACATTTTTGACAACCCTC
	CTCATTTTCAGTTTTTGGATAGCAAGTTTCGTCACCATTTTTGT ACAAACTAAGCATTCCACATTTTTGACAACCCTC
	AGAGGCTGAGATTTTTCTCCTCAAGA
	GCCGAACAAAGTTTTTTTTACCAGAAGCCAAAAGAACTTTTTTG GCATGATTATTACGCAGTATTTTTTGTTAGCAAAC
	GATAGTTGCGCTTTTTCGACAATGA

	CGGAACCGCCTTTTTTCCCTCAGAGCCCACCCTCAGATT TTTGCCGCCACCACAGAGCCGCCGTTTTTCCAGCATTGA
	ACCATTAGCAATTTTTGGCCGGAAAC
2Tet Staples	GAGCCACCACCAGGAGGTTGAGGACGGAATACACCGGAACCA
	CCATCTTTTCATTTTTTAATCAAAATAGTTTATTTTGTTTTTTCA CAATCAA
	TATGGTTTACAAAATCACCAGTAGCACCATTTAGAAAATTCA
	CAGCGCTAAAGTTTTTACAAAAGGGCTATTGACGGAATTTTTTAT TATTCATTCATTTGGGAATTTTTTTAGAGCCAGC
	AAGGTAAAGACATTCAACCGATTGACCACGAACCAGGGAGGG
	ACTTGAGCAAAGGTGAATTATCACAATCAGACAGCGTCACCG
	ACCATTAGCAATTTTTGGCCGGAAAC
	AACCATCGATTAGCCCCCTTATTAGCGTTTGGTCACCAATGA
	TTTCATCGGCATTTTTTTTTCGGTCAAGCAGCACCGTTTTTTAAT CAGTAGCAGTTTGCCTTTTTTTTTAGCGTCAGAC
	CAGAGCCACGCCACCCTCAGAACCCGCGTTGTAGGCCACCCT
	CGGAACCGCCTTTTTTCCCTCAGAGCCCACCCTCAGATTTTTGC CGCCACCACAGAGCCGCCGTTTTTCCAGCATTGA
	AGCCACCACCATAGTTAGCGTAATCTTCATTGCCACCCTCAG
	AGAACCGCCACTTTTTCCTCAGAACCAAAGCCAGAATTTTTTG GAAAGCGCA
	TACCGTTCCATTCTGAAACATGAAAGTATTAGTCTCTGAATT
	GTAAGCGTCATTTTTTACATGGCTTTTAACGGGGTCATTTTTGT GCCTTGAGTGCCTATTTCGTTTTTGAACCTATTA
	ATAAGTTTTGATGATACAGGAGTGCCTGTCAACGTACTGGTA
	ATGCCCCCTAACAGTGCCCGTATAGCCGTTAAGTAACAGTTA
	AGAGGCTGAGATTTTTCTCCTCAAGA
	ATTAGCGGGGAGGTTTAGTACCGCCACCCTCGAAGGATTAGG
	AGGTGTATCACTTTTTCGTACTCAGGTTTTGCTCAGTTTTTTACC AGGCGGACGAGAGGGTTGTTTTTATATAAGTAT
	ACACTGAGCCCAATAGGAACCCATGGAATAGCCCGTACCGTA
	CTCATTTTCAGTTTTTGGATAGCAAGTTTCGTCACCATTTTTGT ACAAACTAAGCATTCCACATTTTTGACAACCCTC
Tetrahedron Staples	TCAGCAGCGAATTTTTAGACAGCATCACAACCATCGCTTTTTC CACGCATAAGTTAAAGGCCGTTTTTCTTTTGCGGG
	GACAATGACAGGAACGAGGGTAGCCACCACCATAGTTGCGCC
	TTCTTAAACAGTTTTTCTTGATACCGCTCATTTTCAGTTTTTGG ATAGCAAGTCAACAGTTTCTTTTTAGCGGAGTGA
	AACAACTAAACAGCTTGCTTTCGAGGTGAATGAATAGAAAGG
	CCTTTAATTGTTTTTTATCGGTTTATGGAATTGCGAATTTTTTA ATAATTTTAAATCTCCAAATTTTTAAAAAAGGCT
	TGCAGGGACCGATATATTCGGTCGAGGAGCCAAACTGAGGCT
	GTAACACTGAGTTTTTTTTCGTCACCGACAACCCTCATTTTTT AGTTAGCGTTTAGTA

	AATGATTTTTATTTTCTGTA
	TCCAGACGAACGATCTAAAGTTTTGTTGATTCACGTCGTCTT
	CCCATGTACCTGGGGTTTTGCTAAACAACTTCCCAATAGGAA
	ATTCCACAAGTACAAACTACAACGCACCCATCGTCCTGTAGC
Pyramid Staples	GAGAGATAACAAAGTAAGCAGATAGCCGAACCGCTAATATCA
	TAATAACGGACACCACGGAATAACTGGTAATAGGAAACGCAA
	AAAGTTACCAGTTTTTAAGGAAACCGAAGTTTTAACGTTTTT GGGTCAGTGC
	TTGCCAGTTAGAATTAACTGAACACCCTGAACTTGAGTAAAT
	CAAAATAAACATTTTTGCCATATTATTTTAACGTCAATTTTTT TTTTTTTTTTTTTTATCGTAGGAA
	TGCTATTTTGCTTTTTACCCAGCTACATAAACAACATTTTTTG TTCAGCTAATTTTTATTTTCTTTTTTTTTTTTTTTTTTTTTAAATG AAAATAGGGAAGCGCATTTTTTTAGACGGGA
	ATTTTTTGTTATCCCAATCCAAATGGCAAAAGGTAAGAAACG
	ATAAAAACAGCAGCCTTTACAGAGATAAGCAATAAGAATAAC
	TTACCGAAGCCTTTTTCTTTTTAAGACCACAAGAATTTTTTTG AGTTAAGCCAGCAAGAAACATTTTTATGAAATAGC
	TGTTAGCAATTAAGACTCCTTATTCTATCAATAGACGCAGTA
	CAAAGTCAGAGTTTTTTTTTTTTTTTTAGTAAATGATGGGGTT TTGTTTTTCTAAACAACT
	AGCATTCCACATTTTTGACAACCCTCCTTTCCAGACGTTTTTTT TTTTTTTTTTTTTGGTAATTGAG
	ATACCCAAAAGTTTTTAACTGGCATGAACGTAGAAAATTTTT TTTTTTTTTTTTTTTGCGTTTTCAT
	CAGACTGTAGCTTTTTTTTTTTTTTTTACATACATACATATAA AAGATTTTTAACGCAAAGA
	CAACGCCTGTTTCAACAGTTTCACCAGCGCTAGTACAAACTA
	GTAACACTGAGTTTTTTTTCGTCACCAAAGACAAAAGTTTTTG GCGACATTC
	GGAGGGAAGGTAAGTGCCGTCGAGAGGGTTGAACCGATTGAG
	TAAATATTGACTTTTTGGAAATTATTTGAAAGTATTATTTTTA GAGGCTGAGTTTTGCTCAGTTTTTTTTTTTTTTTTTTTTCTTT TGCGGG
	TCAGCAGCGAATTTTTAGACAGCATCACAACCATCGCTTTTT CCACGCATAAGTTAAAGGCCGTTTTTTTTTTTTTTTTTTTTA CCAGGCGGA
	CTGAAACACATTAAAGGTCGGAACTCTGTAATTTCTATTATT
	TAGCGGGGACTCCTCAAGAGAAGGGCCACGAACCATTAGGAT
	ATATAAGTATATTTTTTTTTTTTTTTATGGATCTTCGAATGG AAAGCTTTTTGCAGTCTCTG
	CCGCCGCCAGCTTTTTATTGACAGGATTCACAAACGATTT TTTTTTTTTTTTTTTTTTGCCCGGAATA
	GTACTCAGGACCCAATAGGAACCCATGTACCGGTGTATCACC
	CTCATTTTCAGTTTTTGGATAGCAAGGGTTTAGTACCTTT TTGCCACCCTCACCTCAGAACCGTTTTTCCACCCTCAG

	TTTGTCGTATAGTTAGCGTAACGACCACCAGCCATCTAAAGT
	ACCACCAGAGAATTTACCGTTCCATAATAATCCACCAGAACC
	GAGCCACCACCTTTTTCTCAGAGCCGTTTTTCACGTTTTT TTGAAAATCTCC
	CTCCAAAAGGAATCAAGTTTGCCTTTAGCGTAAAAAAAAAGG
	AGCCTTTAATTTTTTTGTATCGGTTTACCATTACCATTTTTTT AGCAAGGCCCACCGTAATCATTTTTTTTTTTTTTTTTTTTTTAT AGAAGGCTTCTAAGAACGTTTTTCGAGGCGTTT
	CCCGACTTGCGTTTTTGGAGGTTTTGAGCAAATCAGATTTTT TTTTTTTTTTTTTTTGTAGCGACAG
	CCAGTAGCATCAGCTTGCTTTCAGAGCCAATTAACAAAATCA
	GATAGCAGGGAAACGTCACCAATGTAATCTTTCAAAACCATC
	GTCATAGCCCCCCTCAGAACCGCCACCCTCACGGCATTTTCG
	CCGCCTCCCTCTTTTTAGAGCCGCCACCTTATTAGCGTTTTTTT TGCCATCTAAAATCACCGGTTTTTAACCAGAGCC
	CCTTGATAGGTTGAGGCAGGTCAGCGGAAACCACACGATTGG
	GACAATGACAGGAACGAGGGTAGCGACGACAAATTTTATCCT
	AAGAACGGTCGGCTGTCTTTCCTTCGGTATTATCATCATTCC
	TGCAGGGACCGATATATTCGGTCGAACCTTAGCGCTGAGGCT
	TTTACGAGAAGAAAAATAATATCCCACCCATCGTCATCCTAA
	CCCAATAGCAAAGCCTTAAATCAAGATTAGTTCATTACCGCG
	CCTGTTTATCTCATCGAGAACAAGCAAGCCGTGCAGAACGCG
	AACAATAGATATTTTTAGTCCTGAACCATGTAGAAACTTTTT CAATCAATAAGTATTAAACCATTTTTAGTACCGCAC

Table 3. *List of all Scaffold strands for all designed nanostructures:*

Tetrahedron Scaffold	CTACCCTCGTTCCGATGCTGTCTTTCGCTGCTGAGGGTGACGA TCCCGCAAAAGCGGCCTTTAACTCCCTGCAAGCCTCAGCGACCG AATATATCGGTTATGCGTGGGCGATGGTTGTTGTCATTGTCGGC GCAACTATCGGTATCAAGCTGTTTAAGAAATTCACCTCGAAAGC AAGCTGATAAACCGATACAATTAAAGGCTCCTTTTGGAGCCTTT TTTTTTGGAGATTTTCAACGTGAAAAAATTATTATTCGCAATTCC TTTAGTTGTTCCTTTCTATTCTCACTCCGCTGAAACTGTTGAAAG TTGTTTAGCAAAACCCCATACAGAAAATTCATTTACTAACGTCT GGAAAGACGACAAAACTTTAGATCGTTACGCTAACTATGAGG GTTGTCTGTGGAATGCTACAGGCGTTGTAGTTTGTACTGGTG ACGAAACTCAGTGTTACGGTACATGGGTTCCTATTGGGCTTG CTATCCCTGAAAATGAGGGTGGTGG

Triangle Scaffold	CTACCCTCGTTCCGATGCTGTCTTTCGCTGCTGAGGGTGA CGATCCCGCAAAAGCGGCCTTTAACTCCCTGCAAGCCTCA GCGACCGAATATATCGGTTATGCGTGGGCGATGGTTGTTG TCATTGTCGGCGCAACTATCGGTATCAAGCTGTTTAAGAAA TTCACCTCGAAAGCAAGCTGATAAACCGATACAATTAAAGG CTCCTTTTGGAGCCTTTTTTTTTGGAGATTTTCAACGTGAAA AAATTATTATTCGCAATTCCTTTAGTTGTTCCTTTCTATTCTCA CTCCGCTGAAACTGTTGAAAGTTGTTTAGCAAAACCCCATAC AGAAAATTCATTTACTAACGTCTGGAAAGACGACAAAACTTT AGATCGTTACGCTAACTATGAGGGTTGTCTGTGGAATGCTAC AGGCGTTGTAGTTTGTACTGGTGACGAAACTCAGTGTTACGG TACATGGGTTCCTATTGGGCTTGCTATCCCTGAAAATGAGGG TGGTGGCTCTGAGGGTGGCGGTTCTGAGGGTGGCGGTTCTG AGGGTGGCGGTACTAAACCTCCTGAGTACGGTGATACACCTA TTCCGGGCTATACTTATATCAACCCTCTCGACGGCACTTATCCG CCTGGTACTGAGCAAAACCCCGCTAATCCTAATCCTTCTCTTGA GGAGTCTCAGCCTCTTAATACTTTCATGTTTCAGAATAATAGGT TCCGAAATAGGCAGGGGGCATTAACTGTTTATACGGGCACTGT TACTCAAGGCACTGACCCCGTTAAAACTTATTACCAGTACACTC CTGTATCATCAAAAGCCATGTATGACGCTTACTGGAACGGTAA ATTCAGAGACTGCGCTTTCCATTCTGGCTTTAATGAAGATCCAT TCGTTTGTGAATATCAAGGCCAATCGTCTGACCTGCCTCAACCT CCTGTCAATGCTGGCGGCGGCTCTGGTGGTGGTTCTGGTGGCG GCTCTGAGGGTGGTGGCTCTGAGGGTGGCGGTTCTGAGGGTG GCGGCTCTGAGGGAGGCGGTTCCGGTGGTGGCTCTGGTTCCG GTGATTTTGATTATGAAAAGATGGCAAACGCTAATAAGGGGG CTATGACCGAAAATGCCGATGAAAACGCGCTACAGTCTGACG CTAAAGGCAAACTTGATTCTGTCGCTACTGATTACGGTGCTGC TATCGATGGTTTCATTGGTGACGTTTCCGGCCTTGCTAATGGT AATGGTGCTACTGGTGATTTTGCTGGCTCTAATTCCCAAATGG CTCAAGTCGGTGACGGTGATAATTCACCTTTAATGAATAATTT CCGTCAATATTTACCTTCCCTCCCTCAATCGGTTGAATGTCGCC CTTTTGTCTTTAGCGCTGGTAAACCATATGAATTTTCTATTGAT TGTGACAAAATAAACTTATTCCGTGGTGTCTTTGCGTTTCTTTT ATATGTTGCCACCTTTATGTATGTATTTTCTACGTTTGCTAACA TACTGCGTAATAAGGAGTCTTAATCATGCCAGTTCTTTTGGGT ATTCCGTTATTATTGCGTTTCCTCGGTTTCCTTCTGGTAACTTT GTTCGGCTATCTGCTTACTTTTCTTAAAAAGGGCTTCGGTAA GATAGCTATTGCT
Crescent Scaffold	CTACCCTCGTTCCGATGCTGTCTTTCGCTGCTGAGGGTGA CGATCCCGCAAAAGCGGCCTTTAACTCCCTGCAAGCCTCA GCGACCGAATATATCGGTTATGCGTGGGCGATGGTTGTTG TCATTGTCGGCGCAACTATCGGTATCAAGCTGTTTAAGAAA TTCACCTCGAAAGCAAGCTGATAAACCGATACAATTAAAGG CTCCTTTTGGAGCCTTTTTTTTTGGAGATTTTCAACGTGAAA

	AAATTATTATTCGCAATTCCTTTAGTTGTTCCTTTCTATTCTCA CTCCGCTGAAACTGTTGAAAGTTGTTTAGCAAAACCCCATAC AGAAAATTCATTTACTAACGTCTGGAAAGACGACAAAACTTT AGATCGTTACGCTAACTATGAGGGTTGTCTGTGGAATGCTAC AGGCGTTGTAGTTTGTACTGGTGACGAAACTCAGTGTTACGG TACATGGGTTCCTATTGGGCTTGCTATCCCTGAAAATGAGGG TGGTGGCTCTGAGGGTGGCGGTTCTGAGGGTGGCGGTTCTG AGGGTGGCGGTACTAAACCTCCTGAGTACGGTGATACACCTA TTCCGGGCTATACTTATATCAACCCTCTCGACGGCACTTATCCG CCTGGTACTGAGCAAAACCCCGCTAATCCTAATCCTTCTCTTGA GGAGTCTCAGCCTCTTAATACTTTCATGTTTCAGAATAATAGGT TCCGAAATAGGCAGGGGGCATTAACTGTTTATACGGGCACTGT TACTCAAGGCACTGACCCCGTTAAAACTTATTACCAGTACACTC CTGTATCATCAAAAGCCATGTATGACGCTTACTGGAACGGTAA ATTCAGAGACTGCGCTTTCCATTCTGGCTTTAATGAAGATCCAT TCGTTTGTGAATATCAAGGCCAATCGTCTGACCTGCCTCAACCT CCTGTCAATGCTGGCGGCGGCTCTGGTGGTGGTTCTGGTGGCG GCTCTGAGGGTGGTGGCTCTGAGGGTGGCGGTTCTGAGGGTG GCGGCTCTGAGGGAGGCGGTTCCGGTGGTGGCTCTGGTTCCG GTGATTTTGATTATGAAAAGATGGCAAACGCTAATAAGGGGG CTATGACCGAAAATGCCGATGAAAACGCGCTACAGTCTGACG CTAAAGGCAAACTTGATTCTGTCGCTACTGATTACGGTGCTGC TATCGATGGTTTCATTGGTGACGTTTCCGGCCTTGCTAATGGT AATGGTGCTACTGGTGATTTTGCTGGCTCTAATTCCCAAATGG CTCAAGTCGGTGACGGTGATAATTCACCTTTAATGAATAATTT CCGTCAATATTTACCTTCCCTCCCTCAATCGGTTGAATGTCGCC CTTTTGTCTTTAGCGCTGGTAAACCATATGAATTTTCTATTGAT TGTGACAAAATAAACTTATTCCGTGGTGTCTTTGCGTTTCTTTT ATATGTTGCCACCTTTATGTATGTATTTTCTACGTTTGCTAACA TACTGCGTAATAAGGAGTCTTAATCATGCCAGTTCTTTTGGGT ATTCCGTTATTATTGCGTTTCCTCGGTTTCCTTCTGGTAACTTT GTTCGGCTATCTGCTTACTTTTCTTAAAAAGGGCTTCGGTAA GATAGCTATTGCT
2Tet Scaffold	CTACCCTCGTTCCGATGCTGTCTTTCGCTGCTGAGGGTGA CGATCCCGCAAAAGCGGCCTTTAACTCCCTGCAAGCCTCA GCGACCGAATATATCGGTTATGCGTGGGCGATGGTTGTTG TCATTGTCGGCGCAACTATCGGTATCAAGCTGTTTAAGAAA TTCACCTCGAAAGCAAGCTGATAAACCGATACAATTAAAGG CTCCTTTTGGAGCCTTTTTTTTTGGAGATTTTCAACGTGAAA AAATTATTATTCGCAATTCCTTTAGTTGTTCCTTTCTATTCTCA CTCCGCTGAAACTGTTGAAAGTTGTTTAGCAAAACCCCATAC AGAAAATTCATTTACTAACGTCTGGAAAGACGACAAAACTTT AGATCGTTACGCTAACTATGAGGGTTGTCTGTGGAATGCTAC AGGCGTTGTAGTTTGTACTGGTGACGAAACTCAGTGTTACGG TACATGGGTTCCTATTGGGCTTGCTATCCCTGAAAATGAGGG

	TGGTGGCTCTGAGGGTGGCGGTTCTGAGGGTGGCGGTTCTG AGGGTGGCGGTACTAAACCTCCTGAGTACGGTGATACACCTA TTCCGGGCTATACTTATATCAACCCTCTCGACGGCACTTATCCG CCTGGTACTGAGCAAAACCCCGCTAATCCTAATCCTTCTCTTGA GGAGTCTCAGCCTCTTAATACTTTCATGTTTCAGAATAATAGGT TCCGAAATAGGCAGGGGGCATTAACTGTTTATACGGGCACTGT TACTCAAGGCACTGACCCCGTTAAAACTTATTACCAGTACACTC CTGTATCATCAAAAGCCATGTATGACGCTTACTGGAACGGTAA ATTCAGAGACTGCGCTTTCCATTCTGGCTTTAATGAAGATCCAT TCGTTTGTGAATATCAAGGCCAATCGTCTGACCTGCCTCAACCT CCTGTCAATGCTGGCGGCGGCTCTGGTGGTGGTTCTGGTGGCG GCTCTGAGGGTGGTGGCTCTGAGGGTGGCGGTTCTGAGGGTG GCGGCTCTGAGGGAGGCGGTTCCGGTGGTGGCTCTGGTTCCG GTGATTTTGATTATGAAAAGATGGCAAACGCTAATAAGGGGG CTATGACCGAAAATGCCGATGAAAACGCGCTACAGTCTGACG CTAAAGGCAAACTTGATTCTGTCGCTACTGATTACGGTGCTGC TATCGATGGTTTCATTGGTGACGTTTCCGGCCTTGCTAATGGT AATGGTGCTACTGGTGATTTTGCTGGCTCTAATTCCCAAATGG CTCAAGTCGGTGACGGTGATAATTCACCTTTAATGAATAATTT CCGTCAATATTTACCTTCCCTCCCTCAATCGGTTGAATGTCGCC CTTTTGTCTTTAGCGCTGGTAAACCATATGAATTTTCTATTGAT TGTGACAAAATAAACTTATTCCGTGGTGTCTTTGCGTTTCTTTT ATATGTTGCCACCTTTATGTATGTATTTTCTACGTTTGCTAACA TACTGCGTAATAAGGAGTCTTAATCATGCCAGTTCTTTTGGGT ATTCCGTTATTATTGCGTTTCCTCGGTTTCCTTCTGGTAACTTT GTTCGGCTATCTGCTTACTTTTCTTAAAAAGGGCTTCGGTAA GATAGCTATTGCT
3Tet Scaffold	CTACCCTCGTTCCGATGCTGTCTTTCGCTGCTGAGGGTGA CGATCCCGCAAAAGCGGCCTTTAACTCCCTGCAAGCCTCA GCGACCGAATATATCGGTTATGCGTGGGCGATGGTTGTTG TCATTGTCGGCGCAACTATCGGTATCAAGCTGTTTAAGAAA TTCACCTCGAAAGCAAGCTGATAAACCGATACAATTAAAGG CTCCTTTTGGAGCCTTTTTTTTTGGAGATTTTCAACGTGAAA AAATTATTATTCGCAATTCCTTTAGTTGTTCCTTTCTATTCTCA CTCCGCTGAAACTGTTGAAAGTTGTTTAGCAAAACCCCATAC AGAAAATTCATTTACTAACGTCTGGAAAGACGACAAAACTTT AGATCGTTACGCTAACTATGAGGGTTGTCTGTGGAATGCTAC AGGCGTTGTAGTTTGTACTGGTGACGAAACTCAGTGTTACGG TACATGGGTTCCTATTGGGCTTGCTATCCCTGAAAATGAGGG TGGTGGCTCTGAGGGTGGCGGTTCTGAGGGTGGCGGTTCTG AGGGTGGCGGTACTAAACCTCCTGAGTACGGTGATACACCTA TTCCGGGCTATACTTATATCAACCCTCTCGACGGCACTTATCCG CCTGGTACTGAGCAAAACCCCGCTAATCCTAATCCTTCTCTTGA GGAGTCTCAGCCTCTTAATACTTTCATGTTTCAGAATAATAGGT TCCGAAATAGGCAGGGGGCATTAACTGTTTATACGGGCACTGT

	TACTCAAGGCACTGACCCCGTTAAAACTTATTACCAGTACACTC CTGTATCATCAAAAGCCATGTATGACGCTTACTGGAACGGTAA ATTCAGAGACTGCGCTTTCCATTCTGGCTTTAATGAAGATCCAT TCGTTTGTGAATATCAAGGCCAATCGTCTGACCTGCCTCAACCT CCTGTCAATGCTGGCGGCGGCTCTGGTGGTGGTTCTGGTGGCG GCTCTGAGGGTGGTGGCTCTGAGGGTGGCGGTTCTGAGGGTG GCGGCTCTGAGGGAGGCGGTTCCGGTGGTGGCTCTGGTTCCG GTGATTTTGATTATGAAAAGATGGCAAACGCTAATAAGGGGG CTATGACCGAAAATGCCGATGAAAACGCGCTACAGTCTGACG CTAAAGGCAAACTTGATTCTGTCGCTACTGATTACGGTGCTGC TATCGATGGTTTCATTGGTGACGTTTCCGGCCTTGCTAATGGT AATGGTGCTACTGGTGATTTTGCTGGCTCTAATTCCCAAATGG CTCAAGTCGGTGACGGTGATAATTCACCTTTAATGAATAATTT CCGTCAATATTTACCTTCCCTCCCTCAATCGGTTGAATGTCGCC CTTTTGTCTTTAGCGCTGGTAAACCATATGAATTTTCTATTGAT TGTGACAAAATAAACTTATTCCGTGGTGTCTTTGCGTTTCTTTT ATATGTTGCCACCTTTATGTATGTATTTTCTACGTTTGCTAACA TACTGCGTAATAAGGAGTCTTAATCATGCCAGTTCTTTTGGGT ATTCCGTTATTATTGCGTTTCCTCGGTTTCCTTCTGGTAACTTT GTTCGGCTATCTGCTTACTTTTCTTAAAAAGGGCTTCGGTAA GATAGCTATTGCT
Pyramid Scaffold	CTACCCTCGTTCCGATGCTGTCTTTCGCTGCTGAGGGTGACG ATCCCGCAAAAGCGGCCTTTAACTCCCTGCAAGCCTCAGCGA CCGAATATATCGGTTATGCGTGGGCGATGGTTGTTGTCATTG TCGGCGCAACTATCGGTATCAAGCTGTTTAAGAAATTCACCT CGAAAGCAAGCTGATAAACCGATACAATTAAAGGCTCCTTTT GGAGCCTTTTTTTTTGGAGATTTTCAACGTGAAAAAATTATTA TTCGCAATTCCTTTAGTTGTTCCTTTCTATTCTCACTCCGCTGA AACTGTTGAAAGTTGTTTAGCAAAACCCCATACAGAAAATTC ATTTACTAACGTCTGGAAAGACGACAAAACTTTAGATCGTTA CGCTAACTATGAGGGTTGTCTGTGGAATGCTACAGGCGTTGT AGTTTGTACTGGTGACGAAACTCAGTGTTACGGTACATGGGTT CCTATTGGGCTTGCTATCCCTGAAAATGAGGGTGGTGGCTCTG AGGGTGGCGGTTCTGAGGGTGGCGGTTCTGAGGGTGGCGGT ACTAAACCTCCTGAGTACGGTGATACACCTATTCCGGGCTATA CTTATATCAACCCTCTCGACGGCACTTATCCGCCTGGTACTGAG CAAAACCCCGCTAATCCTAATCCTTCTCTTGAGGAGTCTCAGCC TCTTAATACTTTCATGTTTCAGAATAATAGGTTCCGAAATAGGC AGGGGGCATTAACTGTTTATACGGGCACTGTTACTCAAGGCAC TGACCCCGTTAAAACTTATTACCAGTACACTCCTGTATCATCAA AAGCCATGTATGACGCTTACTGGAACGGTAAATTCAGAGACT GCGCTTTCCATTCTGGCTTTAATGAAGATCCATTCGTTTGTGAA TATCAAGGCCAATCGTCTGACCTGCCTCAACCTCCTGTCAATG CTGGCGGCGGCTCTGGTGGTGGTTCTGGTGGCGGCTCTGAG GGTGGTGGCTCTGAGGGTGGCGGTTCTGAGGGTGGCGGCT

	CTGAGGGAGGCGGTTCCGGTGGTGGCTCTGGTTCCGGTGA TTTTGATTATGAAAAGATGGCAAACGCTAATAAGGGGGCTAT GACCGAAAATGCCGATGAAAACGCGCTACAGTCTGACGCTAA AGGCAAACTTGATTCTGTCGCTACTGATTACGGTGCTGCTATC GATGGTTTCATTGGTGACGTTTCCGGCCTTGCTAATGGTAAT GGTGCTACTGGTGATTTTGCTGGCTCTAATTCCCAAATGGCTC AAGTCGGTGACGGTGATAATTCACCTTTAATGAATAATTTCCG TCAATATTTACCTTCCCTCCCTCAATCGGTTGAATGTCGCCCTT TTGTCTTTAGCGCTGGTAAACCATATGAATTTTCTATTGATTG TGACAAAATAAACTTATTCCGTGGTGTCTTTGCGTTTCTTTTA TATGTTGCCACCTTTATGTATGTATTTTCTACGTTTGCTAACAT ACTGCGTAATAAGGAGTCTTAATCATGCCAGTTCTTTTGGGTA TTCCGTTATTATTGCGTTTCCTCGGTTTCCTTCTGGTAACTTTG TTCGGCTATCTGCTTACTTTTCTTAAAAAGGGCTTCGGTAAGAT AGCTATTGCTATTTCATTGTTTCTTGCTCTTATTATTGGGCTTAA CTCAATTCTTGTGGGTTATCTCTCTGATATTAGCGCTCAATTACC CTCTGACTTTGTTCAGGGTGTTCAGTTAATTCTCCCGTCTAATG CGCTTCCCTGTTTTTATGTTATTCTCTCTGTAAAGGCTGCTATTT TCATTTTTGACGTTAAACAAAAAATCGTTTCTTATTTGGATTGG GATAAATAATATGGCTGTTTATTTTGTAACTGGCAAATTAGGC TCTGGAAAGACGCTCGTTAGCGTTGGTAAGATTCAGGATAAA ATTGTAGCTGGGTGCAAAATAGCAACTAATCTTGATTTAAGG CTTCAAAACCTCCCGCAAGTCGGGAGGTTCGCTAAAACGCCT CGCGTTCTTAGAATACCGGATAAGCCTTCTATATCTGATTTGC TTGCTATTGGGCGCGGTAATGATTCCTACGATGAAAATAAAA ACGGCTTGCTTGTTCTCGATGAGTGCGGTACTTGGTTTAATA CCCGTTCTTGGAATGATAAGGAAAGACAGCCGATTATTGATT GGTTTCTACATGCTCGTAAATTAGGATGGGATATTATTTTTC TTGTTCAGGACTTATCTATTGTTGATAAACAGGCGCGTTCTG CATTAGCTGAACATGTTGTTTATTGTCGTCG

REFERENCES

[1] P. W. K. Rothemund, (Mar. 2006), "Folding DNA to create nanoscale shapes and patterns,"
Nature, vol. 440, no. 7082, pp. 297–302, Mar. 2006.

[2] D. Han, S. Pal, J. Nangreave, Z. Deng, Y. Liu, and H. Yan, "DNA Origami with Complex Curvatures in Three-Dimensional Space," *Science*, vol. 332, no. 6027, pp. 342–346, Apr. 2011.

[3] E. Oktay *et al.*, "DNA origami presenting the receptor binding domain of SARS-CoV-2 elicit robust protective immune response," *Communications Biology*, vol. 6, no. 1, Mar. 2023.

[4] Q. Jiang, S. Liu, J. Liu, Z. Wang, and B. Ding, "Rationally Designed DNA-Origami Nanomaterials for Drug Delivery In Vivo," *Advanced Materials*, vol. 31, no. 45, p. 1804785, Oct. 2018.

[5] D. Selnihhin, S. M. Sparvath, S. Preus, V. Birkedal, and E. S. Andersen, "Multifluorophore DNA Origami Beacon as a Biosensing Platform," *ACS Nano*, vol. 12, no. 6, pp. 5699–5708, May 2018.

[6] H.-Q. Yu *et al.*, "Recent Advances in Self-Assembled DNA Nanostructures for Bioimaging," vol. 5, no. 10, pp. 4652–4667, May 2022.

[7] R. Rubio-Sánchez, G. Fabrini, P. Cicuta, and L. Di Michele, "Amphiphilic DNA nanostructures for bottom-up synthetic biology," *Chemical Communications*, vol. 57, no. 95, pp. 12725–12740, 2021.

[8] S. Ramakrishnan, H. Ijäs, V. Linko, and A. Keller, (2018), "Structural stability of DNA origami nanostructures under application-specific conditions," *Computational and Structural Biotechnology Journal*, vol. 16, pp. 342–349.

[9] R. Veneziano *et al.*, (Jun. 2016) "Designer nanoscale DNA assemblies programmed from the top down," *Science*, vol. 352, no. 6293, pp. 1534–1534.

[10] Y. Hu, (Oct. 2021) "Self-Assembly of DNA Molecules: Towards DNA Nanorobots for Biomedical Applications," *Cyborg and Bionic Systems*, vol. 2021, pp. 1–3.

[11] Vinod Morya, S. Walia, B. B. Mandal, G. P. Smestad, and D. Bhatia, (Oct. 2020),

"Functional DNA Based Hydrogels: Development, Properties and Biological Applications," *ACS Biomaterials Science & Engineering*, vol. 6, no. 11, pp. 6021–6035.

[12] M. Nishio, K. Tsukakoshi, and K. Ikebukuro,(Apr. 2021) "G-quadruplex: Flexible conformational changes by cations, pH, crowding and its applications to biosensing," *Biosensors and Bioelectronics*, vol. 178, p. 113030.

[13] R. Toy, P. M. Peiris, K. B. Ghaghada, and E. Karathanasis, (Jan. 2014), "Shaping cancer nanomedicine: the effect of particle shape on thein vivojourney of nanoparticles," *Nanomedicine*, vol. 9, no. 1, pp. 121–134.

[14] Maartje M. C. Bastings *et al.*, (May 2018), "Modulation of the Cellular Uptake of DNA Origami through Control over Mass and Shape," *Nano Letters*, vol. 18, no. 6, pp. 3557–3564.

[15] R. Agarwal, V. Singh, P. Jurney, L. Shi, S. V. Sreenivasan, and K. Roy, (Oct. 2013), "Mammalian cells preferentially internalize hydrogel nanodiscs over nanorods and use shape-specific uptake mechanisms," *Proceedings of the National Academy of Sciences*, vol. 110, no. 43, pp. 17247–17252.

[16] Y. Liu, J. Tan, A. Thomas, D. Ou-Yang, and V. R. Muzykantov, (Feb. 2012), "The shape of things to come: importance of design in nanotechnology for drug delivery," *Therapeutic Delivery*, vol. 3, no. 2, pp. 181–194.

[17] P. Zhan, A. Peil, Q. Jiang, D. Wang, S. Mousavi, Q. Xiong, Q. Shen, Y. Shang, B.

[18] S. Dey *et al.*, (Jan. 2021) ,"DNA origami," *Nature Reviews Methods Primers*, vol. 1, no. 1, pp. 1–24.

[19] Heck, Christian. (2018). "Gold and silver nanolenses self-assembled by DNA origami".

[20] E. Torelli *et al.*, "A DNA Origami Nanorobot Controlled by Nucleic Acid Hybridization," *Small*, vol. 10, no. 14, pp. 2918–2926, Mar. 2014.

[21] J. Bush, S. Singh, M. Vargas, E. Oktay, C.-H. Hu, and R. Veneziano, (Jul. 2020) "Synthesis of DNA Origami Scaffolds: Current and Emerging Strategies," *Molecules*, vol. 25, no. 15, p. 3386.

[22] W. E. M. Noteborn, L. Abendstein, and T. H. Sharp, (Dec. 2020), "One-Pot Synthesis of Defined-Length ssDNA for Multiscaffold DNA Origami," *Bioconjugate Chemistry*, vol. 32, no. 1, pp. 94–98.

[23]Veneziano, R., Shepherd, T.R., Ratanalert, S. *et al. In vitro* synthesis of gene-length single-stranded DNA. *Sci Rep* **8**, 6548 (2018).

[24] E. Oktay *et al.*, “Customized Scaffolds for Direct Assembly of Functionalized DNA Origami,” Jun. 2023.

[25] T. C. Lorenz, (May 2012) “Polymerase Chain Reaction: Basic Protocol plus Troubleshooting and Optimization Strategies,” *Journal of Visualized Experiments*, vol. 63, no. 63.

[26] Ana Rita Silva-Santos, Pedro Paulo, Miguel Prazeres. Scalable purification of single stranded DNA scaffolds for biomanufacturing DNA-origami nanostructures: exploring anion-exchange and multimodal chromatography. *Authorea.* March 31, 2022.

[27] P. Corey, “NIST Publishes a Beginner’s Guide to DNA Origami,” (Jan. 08, 2021) *NIST*.

[28] M. Scheible, R. Jungmann, and F. C. Simmel, (2012)“Assembly and microscopic characterization of DNA origami structures,” *Advances in Experimental Medicine and Biology*, vol. 733, pp. 87–96.

[29] B. Bajar, E. Wang, S. Zhang, M. Lin, and J. Chu, (Sep. 2016),“A Guide to Fluorescent Protein FRET Pairs,” *Sensors*, vol. 16, no. 9, p. 1488.

[30] “Fluorescence Resonance Energy Transfer,” (Oct. 02, 2013), *Chemistry LibreTexts*.

[31] G. Bertolin *et al.*, (Jul. 2019), “Optimized FRET Pairs and Quantification Approaches To Detect the Activation of Aurora Kinase A at Mitosis,” *ACS Sensors*, vol. 4, no. 8, pp. 2018–2027.

[32] S. Nummelin, B. Shen, P. Piskunen, Q. Liu, M. A. Kostiainen, and V. Linko, (Jun. 2020) “Robotic DNA Nanostructures,” *ACS Synthetic Biology*, vol. 9, no. 8, pp. 1923–1940.

[33] E. F. Pettersen *et al.*, “UCSF Chimera--A visualization system for exploratory research and analysis,” *Journal of Computational Chemistry*, vol. 25, no. 13, pp. 1605–1612, 2004, doi: https://doi.org/10.1002/jcc.20084.

[34] “tacoxDNA,” *tacoxdna.sissa.it*. http://tacoxdna.sissa.it/

[35] L. Garibyan and N. Avashia, (Mar. 2013)“Polymerase Chain Reaction,” *Journal of Investigative Dermatology*, vol. 133, no. 3, pp. 1–4.

[36] V. T. T. Lan, P. T. T. Loan, P. A. T. Duong, L. T. Thanh, N. T. Ha, and T. B. Thuan, (2012) “Straightforward Procedure for Laboratory Production of DNA Ladder,”

Journal of Nucleic Acids, vol.

[37] D. Shrestha, A. Jenei, P. Nagy, G. Vereb, and J. Szöllősi,(Mar. 2015) "Understanding FRET as a Research Tool for Cellular Studies," *International Journal of Molecular Sciences*, vol. 16, no. 12, pp. 6718–6756.

[38] Y. F. Dufrêne, (Oct. 2002) "Atomic Force Microscopy, a Powerful Tool in Microbiology," *Journal of Bacteriology*, vol. 184, no. 19, pp. 5205–5213.

BIOGRAPHY

Sally Farag came to George Mason University in Fall 2019 as an undergraduate student pursuing a degree in bioengineering. She then joined the accelerated master's program in bioengineering in Fall 2021, where she began working on her Master's degree along with her Bachelors. Sally has always been interested in research and wanted to work with DNA, so she began working with Dr. Rémi Veneziano. She was able to participate in the URSP program at GMU in Summer 2022 to obtain funding for her research in DNA origami. She completed her Bachelor's degree in Fall 2022, and continued to complete her Masters in Summer 2023.